the plant journal

SEB SOCIETY FOR EXPERIMENTAL BIOLOGY

The Plant Journal (2021) doi: 10.1111/tpj.15489

Molecular mechanisms and hormonal regulation underpinning morphological dormancy: a case study using *Apium graveolens* (Apiaceae)

Matthew Walker[1,2], Marta Pérez[1], Tina Steinbrecher[1], Frances Gawthrop[2], Iva Pavlović[3], Ondřej Novák[3], Danuše Tarkowská[3], Miroslav Strnad[3], Federica Marone[4], Kazumi Nakabayashi[1,*] and Gerhard Leubner-Metzger[1,3,*]

[1]*Department of Biological Sciences, Royal Holloway University of London, Egham TW20 0EX, UK,*
[2]*Tozer Seeds, Tozer Seeds Ltd, Cobham KT11 3EH, UK,*
[3]*Laboratory of Growth Regulators, Institute of Experimental Botany, Czech Academy of Sciences and Faculty of Science, Palacký University Olomouc, Olomouc CZ-78371, Czech Republic, and*
[4]*Swiss Light Source, Paul Scherrer Institute, Villigen CH-5232, Switzerland*

Received 6 May 2021; revised 2 September 2021; accepted 6 September 2021.
*For correspondence (e-mail gerhard.leubner@rhul.ac.uk (G.L.-M.); kazumi.nakabayashi@rhul.ac.uk (K.N.)).

SUMMARY

Underdeveloped (small) embryos embedded in abundant endosperm tissue, and thus having morphological dormancy (MD) or morphophysiological dormancy (MPD), are considered to be the ancestral state in seed dormancy evolution. This trait is retained in the Apiaceae family, which provides excellent model systems for investigating the underpinning mechanisms. We investigated *Apium graveolens* (celery) MD by combined innovative imaging and embryo growth assays with the quantification of hormone metabolism, as well as the analysis of hormone and cell-wall related gene expression. The integrated experimental results demonstrated that embryo growth occurred inside imbibed celery fruits in association with endosperm degradation, and that a critical embryo size was required for radicle emergence. The regulation of these processes depends on gene expression leading to gibberellin and indole-3-acetic acid (IAA) production by the embryo and on crosstalk between the fruit compartments. ABA degradation associated with distinct spatiotemporal patterns in ABA sensitivity control embryo growth, endosperm breakdown and radicle emergence. This complex interaction between gibberellins, IAA and ABA metabolism, and changes in the tissue-specific sensitivities to these hormones is distinct from non-MD seeds. We conclude that the embryo growth to reach the critical size and the associated endosperm breakdown inside MD fruits constitute a unique germination programme.

Keywords: *Apium graveolens* (celery), auxin transport, ABA-gibberellin balance, dormancy evolution, embryo growth, endosperm breakdown, morphological dormancy, underdeveloped embryo.

INTRODUCTION

A diversity of seed dormancy mechanisms evolved to time germination and subsequent seedling growth in variable environments (Baskin and Baskin, 2014; Finch-Savage and Footitt, 2017). Seed dormancy is an innate seed characteristic that acts as a block to the completion of germination under conditions that might otherwise be considered favourable for its occurrence if a seed were non-dormant (Finch-Savage and Leubner-Metzger, 2006). As a major determinant of species distribution and habitat selection, seed dormancy may influence evolutionary diversification and adaptation to climatic change (Fernandez-Pascual et al., 2019; Willis et al., 2014). Seed ecologists distinguish several major seed dormancy classes including non-dormancy (ND), physiological dormancy (PD), morphological dormancy (MD) and morphophysiological dormancy (MPD) (Baskin and Baskin, 2014; Willis et al., 2014). These are associated with functional traits underlying the variation in germination phenology in adaptation to seasons, climates and habitats (Fernandez-Pascual et al., 2019; Finch-Savage and Footitt, 2017). An abundance of published work has revealed the underpinning molecular mechanisms of PD (e.g. *Arabidopsis thaliana*, Brassicaceae) and ND (e.g. *Lepidium sativum*, Brassicaceae) seeds in response to environmental cues (Chahtane et al., 2017; Finch-Savage and Footitt, 2017; Graeber et al., 2014;

Linkies et al., 2009; MacGregor et al., 2015; Nonogaki, 2019; Shu et al., 2016; Yan et al., 2014). This comprehensive molecular research with PD and ND seeds revealed that the antagonistic interaction between the hormones ABA and gibberellins (GAs) constitutes the central node of the hormonal network controlling dormancy and germination in response to the environment. ABA is the key positive regulator for dormancy induction and maintenance, whereas GAs are involved in dormancy release and the promotion of germination. They act antagonistically in regulating the embryo's growth potential and the constraint weakening of tissues covering the radicle (micropylar endosperm, coleorhiza, micropylar seed (testa), or fruit (pericarp) coat) (Holloway et al., 2021; Steinbrecher and Leubner-Metzger, 2018; Yan et al., 2014). Recent work demonstrated that auxins, with indole-3-acetic acid (IAA) as the major bioactive molecule, are also a key regulator in PD seeds (Matilla, 2020; Pellizzaro et al., 2020; Shu et al., 2016).

By contrast to PD and ND seeds, the molecular mechanisms underpinning morphological dormancy in species with MD and MPD seeds are largely unknown. This lack of knowledge is especially obstructive because both MD and MPD have been proposed to constitute the ancestral state in seed dormancy evolution (Baskin and Baskin, 2014; Baskin et al., 2006; Forbis et al., 2002; Willis et al., 2014) and PD and ND seeds therefore constitute seeds with derived mechanisms. The hallmark of seeds with morphological dormancy is an underdeveloped (small) embryo embedded in abundant endosperm tissue (Figure 1) at the time of maturity and dispersal. The underdeveloped embryo in MD/MPD must first grow inside the imbibed seeds before germination can be completed by radicle emergence (de Farias et al., 2015; Homrichhausen et al., 2003; Jacobsen and Pressman, 1979; Jacobsen et al., 1976; Porceddu et al., 2017; da Silva et al., 2008; Van der Toorn and Karssen, 1992; Zhang et al., 2019). This embryo growth within the seed occurs at the expense of the endosperm, which is dissolved and absorbed by the embryo to fuel its growth. Although the approximately 12% of species with MD/MPD are widespread across the phylogenetic tree of seed plants, they are clearly dominant among basal angiosperm clades and rare within the Rosids, which include the Brassicaceae (Baskin et al., 2006; Finch-Savage and Leubner-Metzger, 2006; Forbis et al., 2002; Willis et al., 2014). In agreement with the finding that seeds with small embryos represent the ancestral state, synchrotron radiation X-ray tomographic microscopy (SRXTM) of fossil seeds from the Early Cretaceous revealed that these extinct angiosperms had small embryos embedded within abundant nutrient storage tissue (Friis et al., 2015). The rapid radiation and diversification of the angiosperms occurred during the Cretaceous period ('Darwin's abominable mystery') with seed traits among the adaptations to diverse environments.

The crown group age of both the Brassicales with PD/ND seeds containing large embryos (including the Arabidopsis and Lepidium model systems) and the Apiales with mainly MD/MPD seeds containing small embryos is in the Late Cretaceous (Calvino et al., 2016; Li et al., 2019; Vandelook et al., 2012; Wen et al., 2020). The Apiaceae (carrot family) is an advanced Asterid family with approximately 430 genera divided into four monophyletic subfamilies harbouring many important food and spice plants (Figure 1). This includes *Apium graveolens* (celery) for which earlier work provided insight into the physiology of the GA-induced endosperm degradation in MD fruits (Dwarte and Ashford, 1982; Jacobsen and Pressman, 1979; Jacobsen et al., 1976). Furthermore, work with *Daucus carota* (carrot) identified an endo-β-1,4-mannanase (DcMAN1) involved in the degradation of the mannan-rich Apiaceae endosperm cell walls to aid embryo growth (Homrichhausen et al., 2003). We show here that the Apiaceae provide excellent model systems for MD/MPD and that our study species celery is an excellent model for investigating the molecular and hormonal mechanisms of MD.

RESULTS

The ancestral seed state with underdeveloped embryos is retained in the Apiaceae

Figure 1 shows that the mature diaspores (seeds or fruits) of all investigated Apiaceae species have small (underdeveloped) embryos, and thus the seeds have MD or MPD. The Apiaceae dispersal units are dry single-seeded indehiscent fruit halves (mericarps, hereafter called fruits) with a dead outer pericarp-testa (fruit and seed coat) layer (Figure 1a). The small embryo is embedded in an abundant living endosperm that occupies most of the fruit's inner space. In the fruits of most of the Apiaceae food and spice plants, the small embryo is linear and well developed into embryonic root (radicle) and shoot (Figure 1a). Both MD and MPD require that the small embryo first grows inside the seed before it can complete germination by radicle emergence (Baskin and Baskin, 2014; Zhang et al., 2019). By contrast to MD seeds, MPD seeds are physiologically dormant and require an additional dormancy-breaking pretreatment to initiate this embryo growth. Figure 1b shows that all the approximately 180 investigated Apiaceae species have either MD or MPD (Data S1). Eight levels, distinguished by the required temperature regime of the pretreatment, are known for the MPD class. In addition to MD, six of these MPD levels are found in the Apiaceae (Data S1). Based on its phylogenetic placement and evolutionary history (Figure 1), the available genome sequence (Li et al., 2020) and the absence of physiological dormancy, *Apium graveolens* (celery) fruits provide an excellent system for

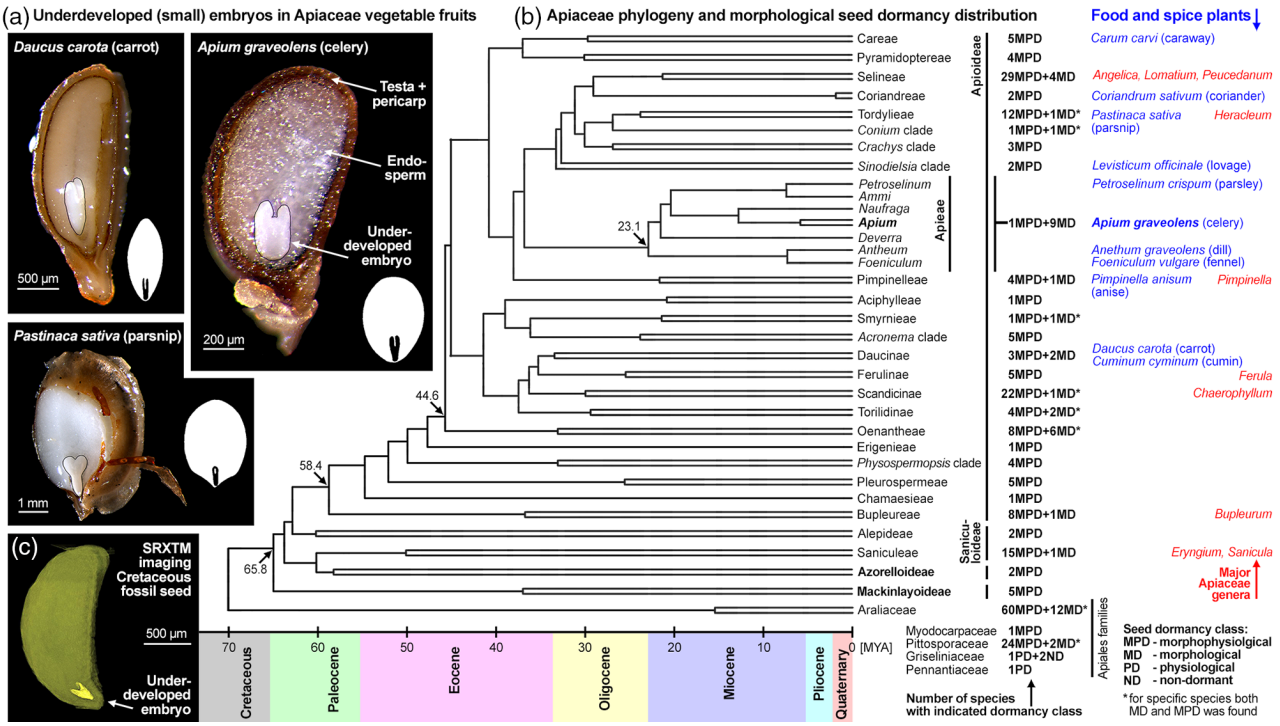

Figure 1. Phylogeny and morphological dormancy of the Apiaceae (carrot family). (a) Mericarps (hereafter called fruits) of three Apiaceae vegetable crops showing underdeveloped (small) embryos embedded in abundant living endosperm tissue; pictograms from Martin (1946). (b) Molecular phylogeny of the Apiaceae, distribution and number of species with morphological (MD) and morphophysiological (MPD) dormancy, and important food and spice plants. The simplified phylogenetic tree representing the four monophyletic subfamilies (Apioidea, Saniculoideae, Azorelloideae, Mackinlayoideae) and the major Apiaceae tribes (including the Apieae) was generated by reducing species-rich molecular phylogenetic trees (Calvino et al., 2016; Vandelook et al., 2012) to tribe level and by adjusting the estimated divergence times (MYA, million years ago) of these tribes to the newest estimates (Vandelook et al., 2012; Wen et al., 2020). The distribution and number of species with specific seed dormancy classes was associated with this phylogenetic tree using information from the book *Seeds* (Baskin and Baskin, 2014) and by extending this with additional information from the published literature as compiled in Data S1 and described in detail in the SI Methods. (c) Synchrotron radiation X-ray tomographic microscopy image of an Early Cretaceous angiosperm fruit with small embryo from Friis et al. (2015); reproduced with permission.

investigating the molecular mechanisms and hormonal regulation underpinning MD in the absence of an interfering physiological dormancy component.

Embryo growth and endosperm degradation inside imbibed celery fruits

Figure 2 shows that growth of the small embryos occurred inside imbibed celery fruits within 5–6 days and preceded the completion of germination scored by visible pericarp rupture and radicle emergence. To consider a possible effect of the fruit size variation, we used the embryo-fruit (E:F) length ratio to quantify the embryo growth and define the value achieved at 50% radicle emergence of the population as the critical E:F ratio required for the completion of germination. Just after the start of imbibition, the E:F length ratio was 0.29 ± 0.01 (Figure 2). After a short lag phase of approximately 1 day, the embryo grew approximately 3-fold to achieve the critical E:F ratio of 0.82 ± 0.01 ($P < 0.0001$). The same pattern of embryo growth and similar critical E:F ratios were obtained with several celery cultivars (Figure S1). The critical E:F ratio was associated with subsequent radicle emergence (day 5–7), with a maximum germination percentage of approximately 98% achieved by 10 days (Figure 2b). To investigate an increase in the embryo growth potential, embryos were extracted from fruits imbibed for 1–5 days and the growth of the isolated embryos over a 9-day incubation period was analysed (Figure 2c). Isolated embryos did not appreciably increase in length when extracted from fruits that had been imbibed for 1 or 2 days ($P > 0.05$). Isolated embryos increased in length by 22.0, 48.5 and 59.5% when extracted from fruits imbibed for 3, 4 and 5 days, respectively. The observed increase in the embryo growth potential was most pronounced between days 2/3 and 3/4 of fruit imbibition (Figure 2c). These patterns define three phases (Figure 2): (I) fruit imbibition and initiation of embryo growth; (II) embryo growth inside the fruit towards a critical E:F ratio; and (III) completion of germination by pericarp rupture and radicle emergence associated with growth beyond the critical E:F ratio.

We further analyzed embryo growth within the fruit using SRXTM imaging (Figure S2). Comparison of virtual sections of a dry (Figure S2a,c,e) and 5-day imbibed fruit

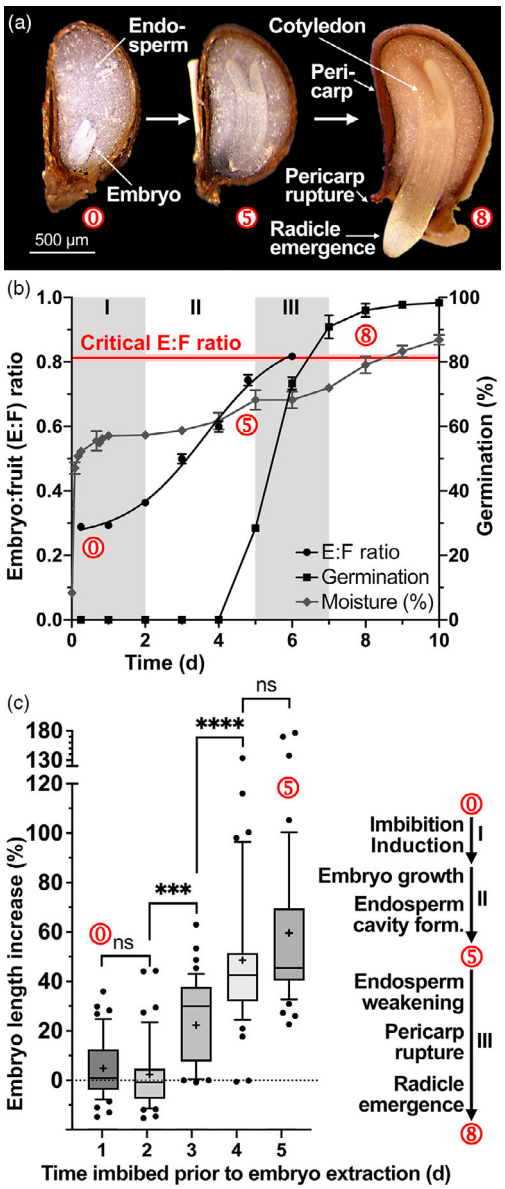

Figure 2. Embryo growth and germination kinetics of celery fruits. (a) Microscopic images of *Apium graveolens* cv. Victoria mericarps (hereafter termed fruits) showing the growth of the small embryo from the start of imbibition to day 5 (to) and a germinated fruit on day 8 (). (b) Progression of embryo growth inside the fruit and germination during incubation at 20°C in continuous light. Embryo growth within fruits was scored as embryo:fruit (E:F) ratios calculated from the embryo and fruit lengths. The critical E:F ratio represents the embryo growth threshold value at which radicle protrusion occurs. Values are the mean ± SEM (n = 50). The sigmoidal non-linear regression curve fitted to the E:F ratio data had a goodness of fit r^2 value of 0.8352 and $P < 0.0001$. (c) Growth potential of embryos extracted from fruits imbibed for 1–5 days and subsequently incubated for 9 days as isolated embryos. Box plots with 10–90 percentiles of percentage increase in embryo length are presented (n = 48). Significance was inferred using one-way analysis of variance (****$P < 0.001$; ***$P < 0.01$; ns, not significant).

(Figure S2b,d,f) showed that the approximately 3-fold increase in embryo length was a result of both hypocotyl and cotyledon growth, although most of the growth appears to occur within the hypocotyl. The SRXTM images suggest that achieving the embryo growth also included cell division, which is consistent with earlier work using classical microscopy (Van der Toorn and Karssen, 1992). This work demonstrated that embryo growth during phase I and early phase II was mainly by cell expansion, whereas embryo growth from day 3 onwards (phase II and III) was dominated by cell division with an approximately 1.5-fold increase in embryo cell number. Figure S2d shows that the progression of endosperm breakdown and expansion of a cavity within the endosperm begins adjacent to the embryo, with endosperm cells becoming partially degraded and depleted, and irregular in shape. These cells were also visibly losing their aleurone grains (protein bodies, AL in Figure S2d), as described previously (Dwarte and Ashford, 1982). The cells of the micropylar endosperm surrounding the radicle were smaller and different in shape compared to the distal endosperm regions and, on day 5, also appeared to be partially degraded and depleted (Figure S2f). The thickness of the micropylar endosperm layer did not change during fruit imbibition (Figure S1). The living endosperm of celery fruits is surrounded by a thin testa and a thick pericarp tissue, which both consist of dead cells (Figure S2). Manual removal of the micropylar pericarp resulted in faster and more uniform germination, whereas removal of the distal pericarp did not result in enhanced germination performance (Figure S3). Taken together, this suggests that constraint weakening of the micropylar endosperm and pericarp may be required for pericarp rupture and radicle emergence (Figure 2).

Distinct regulation of celery embryo growth, endosperm degradation and germination by GA and ABA

To investigate how plant hormones control embryo growth inside celery fruits, we utilized a combined approach consisting of the spatiotemporal analysis of endogenous hormone and gene expression patterns with pharmacological experiments. Figure 3 shows that treatment of celery fruits with 100 µM gibberellin (GA_{4+7}) does not appreciably affect embryo growth and only slightly promoted germination in that the time to reach 50% radicle emergence ($t_{50\%}$) was 0.5 days earlier ($P < 0.05$). Treatment with the GA biosynthesis inhibitor flurprimidol (FLP) had a profound effect in that it completely blocked embryo growth (Figure 3a) and germination (Figure 3b). The combined treatment (GA + FLP) fully restored germination confirming the specificity of the GA biosynthesis inhibitor's action and the requirement of bioactive GA for celery embryo growth and germination.

Treatment of celery fruits with 100 µM ABA inhibited embryo growth leading to a mean E:F ratio of 0.74 on day 6, which is 90% of the control value (Figure 3a). By contrast to this small effect on embryo growth, 100 µM ABA strongly inhibited germination in that it delayed radicle emergence and reduced the maximum germination

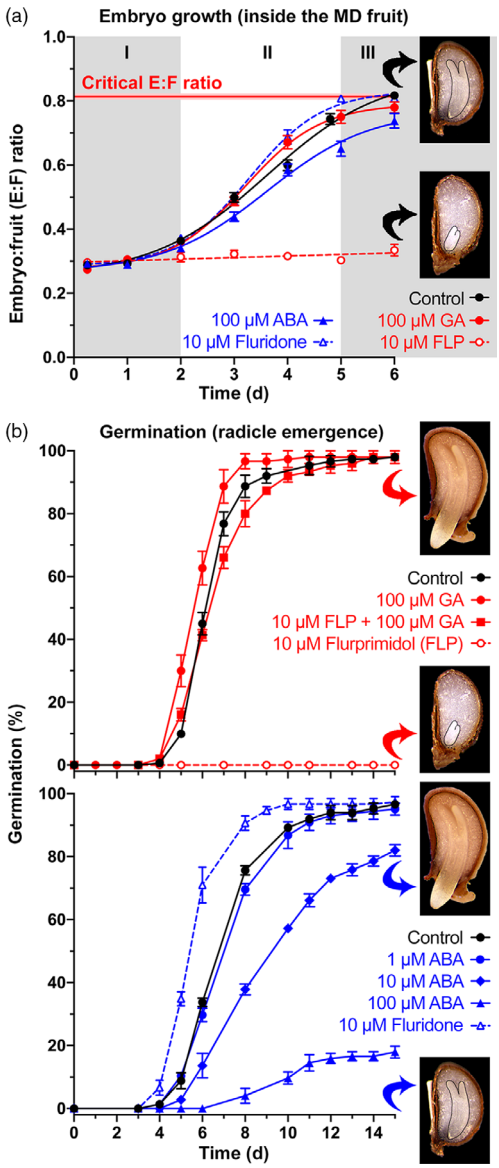

Figure 3. Embryo growth and germination responses to gibberellin (GA), ABA and biosynthesis inhibitors. (a) Embryo growth of *Apium graveolens* cv. Victoria during the incubation of imbibed fruits at 20°C in continuous light. Fruits were incubated without (control) or with GA_{4+7}, ABA, fluridone or flurprimidol (FLP) added at the concentrations indicated. Embryo growth within fruits was scored as embryo:fruit (E:F) ratios and non-linear regression curve fitting as described in Figure 2. Goodness of fit r^2 values: control, 0.835; GA, 0.800; ABA, 0.691; fluridone, 0.851; Hill slope coefficient (nH) describing the steepness of the fitted model: control, 0.46; GA, 0.61; ABA, 0.45; fluridone, 0.63; FLP was fitted with a linear regression and did not differ significantly from zero ($P > 0.05$). The critical E:F ratio of the control is indicated. Fruit images with outlined embryo sizes at the right indicate the effects of the compounds on the embryo growth observed during the incubation. Values are the mean ± SEM ($n = 50$). (b) Effects of GA, ABA and their biosynthesis inhibitors on the germination of fruits scored as radicle emergence. The mean ± SEM values of three plates each with 50 fruits are presented.

percentage to 20% (Figure 3c). Inhibiting ABA biosynthesis with fluridone (Chahtane et al., 2017) slightly promoted celery embryo growth (Figure 3a) and fluridone also promoted germination in that $t_{50\%}$ was approximately 1 day earlier ($P < 0.05$) (Figure 3c). A more detailed comparison of the embryo size variations demonstrated that, on day 1 (0.29 ± 0.05; mean ± SD) and day 6 (control: 0.82 ± 0.07; fluridone: 0.81 ± 0.05), their normal distributions were defined by very similar values. By contrast to this, the day 6 embryo sizes from the 100 µM ABA series did not exhibit normal distribution (Figure 4a). More than 70% of the ABA treated embryos were smaller than the mean value (0.74) and represent the non-germinating fraction. The germinating ABA fraction (approximately 20% in 100 µM ABA) is part of the embryo population with embryo sizes within the critical size range of the control (Figure 4a). By contrast to embryo size (Figure 4a), the completion of germination by radicle protrusion was inhibited by 10 µM ABA and promoted by fluridone (Figure 3).

Because ABA slightly inhibited embryo growth and strongly inhibited germination (Figure 3), ABA degradation is expected to occur during fruit imbibition. To investigate this, ABA contents were quantified in whole fruits, as well as in the major fruit compartments (embryo, endosperm and pericarp). Figure 4d shows that the ABA content in dry fruits was very high (>4000 pmol g^{-1}) and declined rapidly upon imbibition. A approximately 13-fold decline was evident on day 1 to approximately 290 pmol g^{-1}, and there was a further decline to approximately 170 pmol g^{-1} (day 3) and approximately 150 pmol g^{-1} (day 5) in germinated fruits. Most of this ABA was in the pericarp, with the contents in the endosperm and embryo compartments being much lower (Figure 4d). Phaseic acid (PA) and dihydrophaseic acid (DPA) were detected as major ABA degradation products in dry fruits and germinating fruits (Figure 4f). Consistent with a rapid decline in ABA content, the transcript abundances for the key ABA biosynthesis 9-*cis*-epoxycarotenoid dioxygenase genes (*AgrNCED2*, *AgrNCED6* and *AgrNCED9*) declined (Figure 4e, Figure S4). The transcript abundances for *AgrCYP707A1* increased 4-fold with a transient peak on day 3, and those of *AgrCYP707A2* were high in dry fruits and declined upon imbibition (Figure 4e). The rapid decline of ABA upon imbibition may therefore be achieved by ABA 8′-hydroxylase activity present in the dry fruit (*AgrCYP707A2*) and the further decline by *de novo* production of *AgrCYP707A1*. The expression of the two *CYP707A* genes was mainly associated with the endosperm (Figure 4e). The *AgrCYP707A1* peak value on day 3 was downregulated by ABA and upregulated by GA treatment (Figure 5f), suggesting that feedback regulation plays a role in the control of ABA degradation.

ABA and GA both play important roles in the control of celery fruit germination in the light, and this was even more pronounced when fruits were imbibed in darkness (Figure 5g). Celery fruit germination requires light and no germination was observed after 3 weeks of incubation in darkness. Only the combined treatment with GA plus fluridone was effective to fully restore maximum germination

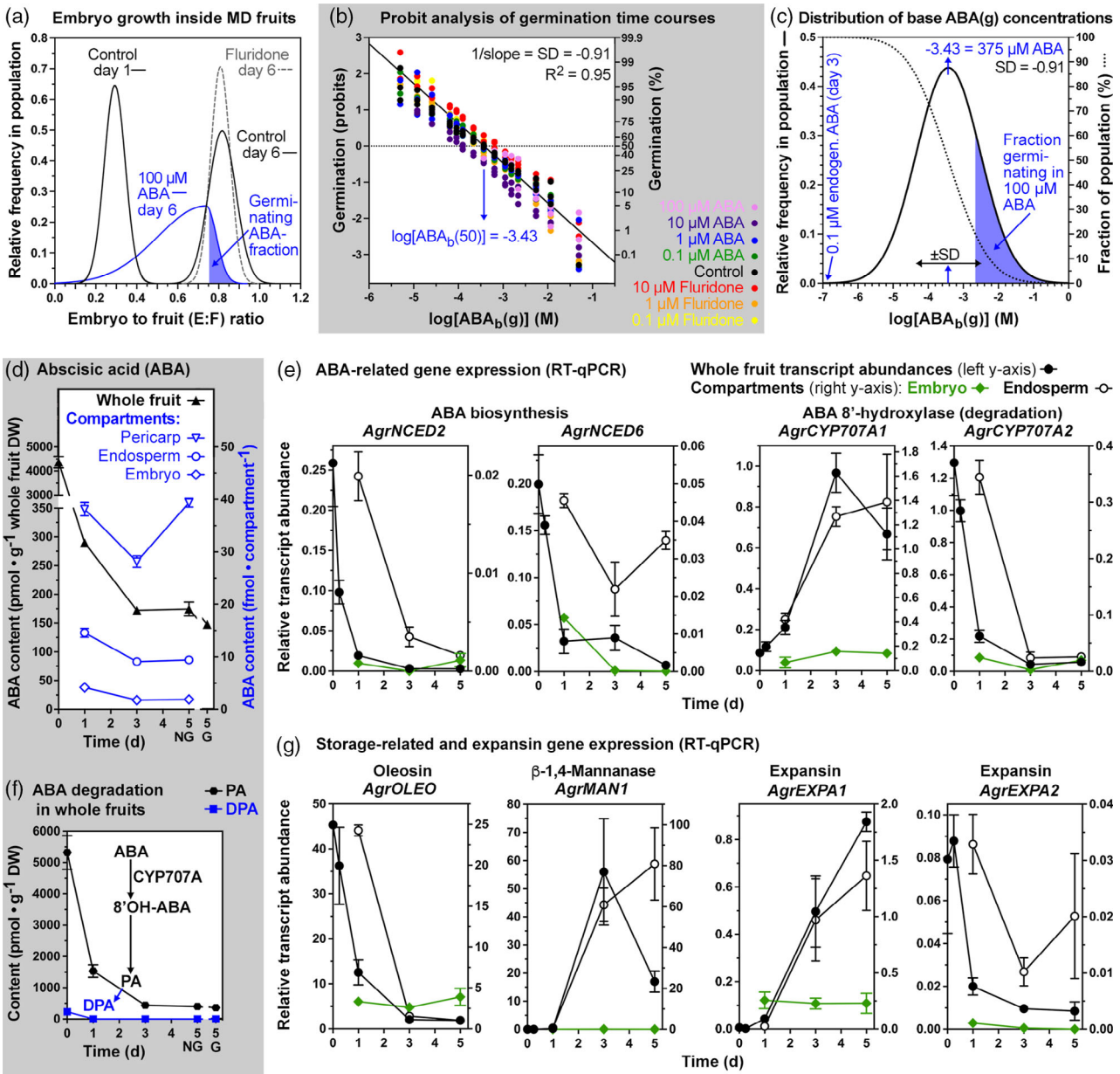

Figure 4. ABA sensitivity modelling, metabolite profiling and gene expression during embryo growth and germination of celery fruits. (a) Analysis of embryo size variation presented as the mean ± SD for control and 10 µM fluridone. For 100 µM ABA, the embryo sizes were not normally distributed: > 70% were smaller than the mean with SD 0.24 (left side only) and the remaining approximately 30% were larger than the mean with SD 0.05 (right side only). (b) Probit analysis of ABA and fluridone responses; details of the population-based threshold modelling are presented and described in Figure S5. (c) Distribution of ABA threshold concentrations in the fruit population (for details, see Figure S5). (d) Spatiotemporal patterns of ABA in *Apium graveolens* cv. Victoria during the incubation of imbibed fruits at 20°C in continuous light. ABA was quantified in whole fruits, as well as in fruit compartments: the dead pericarp tissue, the living endosperm and embryo. (e) Whole fruit and compartment-specific relative transcript abundance patterns [reverse transcription quantitative real-time PCR (RT-qPCR)] during celery fruit imbibition in continuous light for key genes in ABA biosynthesis and degradation: 9-*cis*-epoxycarotenoid dioxygenases (*AgrNCED2* and *AgrNCED6*) and ABA 8′-hydroxylases (*AgrCYP707A1* and *AgrCYP707A2*); for additional ABA-related genes, see Figure S4. (f) Metabolites of the CYP707A-associated ABA degradation pathway: phaseic acid (PA) and dihydrophaseic acid (DPA). (g) Relative transcript abundance patterns (RT-qPCR) of storage-related and expansin genes. The mean ± SEM values of five (metabolites) or three (RT-qPCR) biological replicate samples are presented. NG, not germinated; G, germinated.

in darkness (Figure 5g). It therefore appears that light-induced upregulation of GA biosynthesis combined with ABA degradation is required in the early phase to induce and maintain embryo growth and endosperm breakdown, as well as in the late phase to complete radicle emergence, which is strongly inhibited by ABA. Our finding that treatment with the GA biosynthesis inhibitor flurprimidol blocked embryo growth and germination in the light and can be reversed by GA treatment (Figure 3) directly demonstrates the GA biosynthesis requirement.

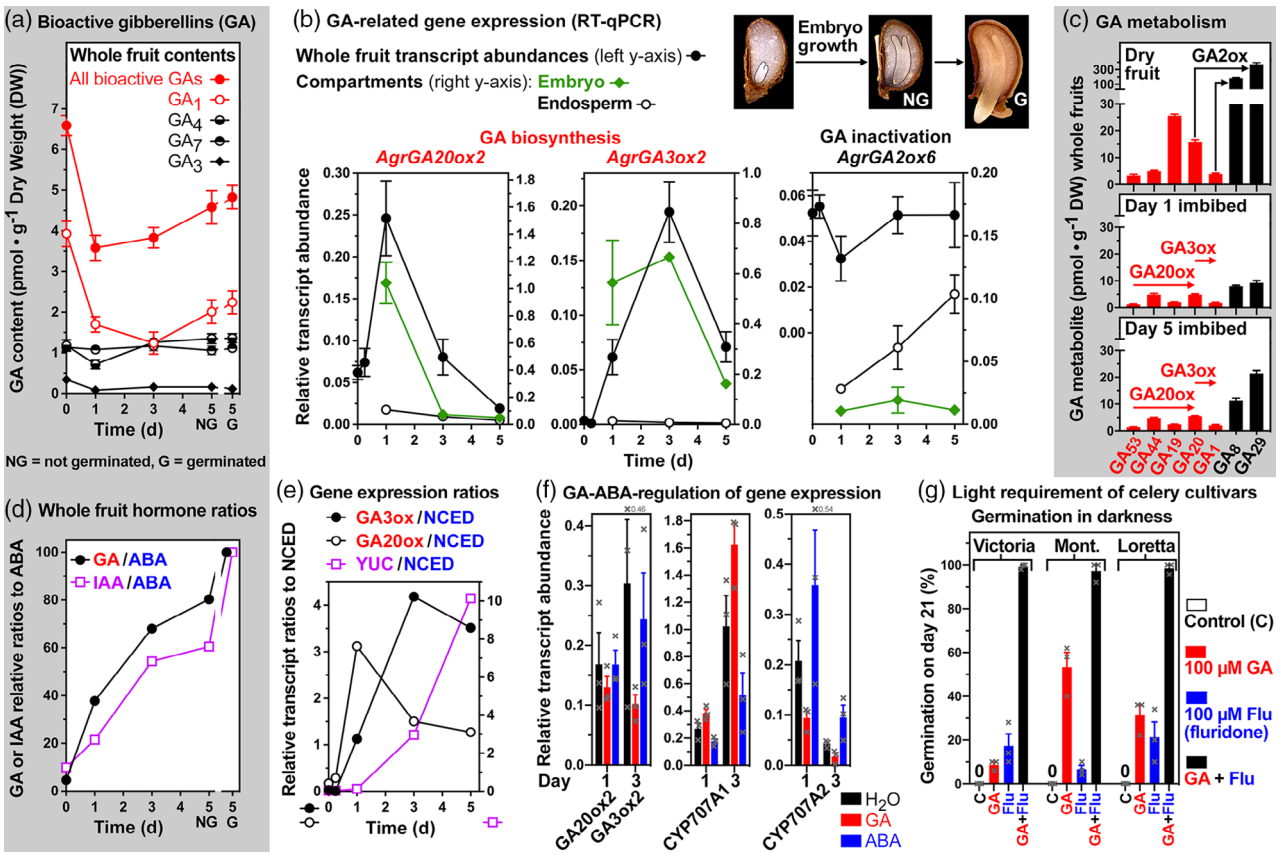

Figure 5. Gibberellin (GA) metabolite profiling and GA-related gene expression during embryo growth and germination of celery fruits. (a) Temporal patterns of bioactive gibberellins (GA) in *Apium graveolens* cv. Victoria during the incubation of imbibed fruits at 20°C in continuous light. Note that, at day 5, not germinated (NG) and germinated (G) fruits were analysed separately. The mean ± SEM values of five biological replicate samples each with approximately 100 fruits are presented. (b) Whole fruit and compartment-specific relative transcript abundance patterns [reverse transcription quantitative real-time PCR (RT-qPCR)] during celery fruit imbibition in continuous light for key genes in GA-biosynthesis and GA-inactivation: GA 20-oxidase *AgrGA20ox2*, GA 3-oxidase *AgrGA3ox2* and GA 2-oxidase *AgrGA2ox6*; for additional GA-related genes, see Figure S3. The mean ± SEM values of three biological replicate RNA samples each obtained from approximately 100 whole fruits, 600 embryos (day 1), 300 embryos (days 3 and 5) or 200–300 endosperms are presented. Images of fruits depict embryo growth and germination. (c) Metabolites of the GA 13-hydroxylation pathway in dry fruits compared to fruits imbibed in the light (days 1 and 5); key enzymes are indicated. For a list of all GA metabolites quantified, see Table S1. (d) Molar ratios of bioactive hormones and (e) key hormone biosynthesis genes in celery fruits. (f) Regulation of GA biosynthesis and ABA degradation gene expression (RT-qPCR) by the addition of either 100 µM GA_{4+7} (GA) or 100 µM ABA to celery fruits imbibed in continuous light. (g) Light requirement of celery fruit germination investigated for three cultivars by fruit incubation in darkness; final germination percentages after 3 weeks are presented. Note that no germination occurred in darkness (control) and that only the combination treatment with 100 µM GA_{4+7} (GA) plus fluridone (to inhibit ABA biosynthesis) resulted in full germination in darkness. The mean ± SEM values of three plates each with 50 fruits are presented.

If GA biosynthesis is indeed required in the early phase to promote embryo growth, then an increase in bioactive GAs should be initiated upon imbibition. To investigate this, individual metabolites of the GA pathway in whole fruit were quantified (Figure 5, Table S1). We found that the 13-hydroxylated biosynthetic pathway leading to GA_1 as bioactive GA was dominant in celery fruits and large amounts of GA_8 and GA_{29} accumulated in dry fruits (Figure 5c), although the GA_1 contents declined upon imbibition and increased only late in the phase (Figure 5a). The sum of all detected bioactive GAs also exhibited an initial rapid approximately 2-fold decline upon imbibition and subsequently increased approximately 1.5-fold during the late phase of embryo growth (Figure 5a). The analysis of the GA metabolites in dry fruits (Figure 5c) suggested predominant GA inactivation by GA 2-oxidases (GA2ox) compared to GA biosynthesis occurred during celery late fruit maturation and drying. Upon fruit imbibition, this rapidly switched towards enhanced GA synthesis by GA 20-oxidases (GA20ox) and GA 3-oxidases (GA3ox), leading to the approximately 1.5-fold increase in bioactive GAs during the late phase of embryo growth (Figure 5a,c).

Consistent with increased bioactive GA levels, induction of celery *GA20ox* and *GA3ox* was observed in whole fruits (Figure 5b and Figure S4). The transcript abundances in embryo and endosperm showed that the upregulation of GA biosynthetic gene expression was associated with the embryo, whereas their expression in the endosperm was comparatively low or declining. By contrast, expression of *AgrGA2ox6* was associated with the endosperm (Figure 5b). The increase

in the bioactive GA content during the late phase of embryo growth and fruit germination (II and III) therefore appears to originate from GA biosynthesis by the embryo.

In agreement with this and the observed requirement for embryo-associated upregulation of GA biosynthesis combined with enhanced ABA degradation, the GA/ABA ratio increased steadily (Figure 5d). A rapid approximately 8-fold increase in the GA/ABA ratio occurred upon imbibition (dry state to day 1) and reached approximately 20-fold on day 5. This spatiotemporal switch from ABA to GA during embryo growth and endosperm degradation may be associated with changes in hormone sensitivities. To quantify their sensitivities, we conducted population-based threshold modelling (Bradford et al., 2008; Ni and Bradford, 1992; Still and Bradford, 1998) of the germination responses to treatments with different hormone concentrations (Figure 3). The modelling results for ABA are presented in Figure S5 and details of how the analyses were conducted are provided. This included probit analysis, which, for ABA, delivered a mean base concentration reducing germination to 50% [$ABA_b(50)$] of 375 μM (SD 0.91) (Figure 4b; for details of the ABA analysis, see Figure S5a–c). Using these values, Figure 4c shows how the threshold $ABA_b(g)$ is distributed among celery fruits in the population. It also shows that the approximately 20% fraction of fruits germinating in the presence of 100 μM ABA have larger embryos (Figure 4a) combined with high threshold values ($ABA_b > 2$ mM) and that the decrease in endogenous ABA on day 3 (approximately 0.1 μM) permits the germination of all fruits (Figure 4c). Furthermore, when the model was applied to the germinating promoting effect of 10 μM fluridone, the inhibitor generates a response that corresponds to the endogenous ABA concentration on day 3 (Figure S5a). The complete block obtained by 1 μM flurprimidole demonstrates that GA biosynthesis is required for germination, and the full germination response of the control (Figure 3) suggests that the endogenous GA concentration on day 3 (approximately 2.5 nM) is already saturating. Taken together with the fact that GA biosynthesis is required for germination (Figure 3), the findings suggest that the steadily increasing GA/ABA ratio (Figure 5d) and tissue-specific spatial differences in the GA and ABA sensitivities may determine the responses.

Auxin biosynthesis and transport during celery embryo growth and germination

Auxin is known to regulate many aspects of seed development and determines the size and weight of crop seeds (Cao et al., 2020; Matilla, 2020; Pellizzaro et al., 2020). Figure 6a shows that the IAA content in celery fruits rapidly declined approximately 7-fold upon imbibition (day 1) and subsequently increased approximately 2-fold during embryo growth (phase II) and radicle emergence (phase III). Most of this IAA was localised in the endosperm, where its levels remained roughly constant over the study period. By contrast, the IAA contents within the embryo increased approximately 8-fold in association with its growth (Figure 6a).

Key genes in the major tryptophan-dependent IAA biosynthesis pathway, such as *TAR2* tryptophan aminotransferase and *YUCCA* flavin monooxygenases (Kasahara, 2016), exhibited spatiotemporal expression patterns well-correlated with the observed IAA contents in imbibed celery fruits (Figure 6b, Figure S4). Transcript accumulation for *AgrTAR2*, *AgrYUC1*, *AgrYUC10*, *AgrYUC3*, and *AgrYUC7* was observed from day 3 onwards during embryo growth and germination. The sum of these four *YUC* transcript abundance increased approximately 15-fold in the embryo from day 1 to day 5 (Figure 6b). Expression of the *TAR2* and *YUC* genes was confined to the embryo and remained very low in the endosperm (Figure 6b, Figure S4). The contents of the major IAA degradation and conjugation products 2-oxoindole-3-acetic acid (oxIAA) and IAA-aspartic acid remained roughly constant in ungerminated fruits between days 1 and 5, then decreased significantly, approximately 30-fold for oxIAA, in germinated fruits on day 5 (Figure 6c). These IAA degradation and conjugation compounds were localised exclusively in the endosperm (Figure S6b) suggesting that during seed development the endosperm was a major compartment for IAA metabolism, which also led to the high IAA contents in dry fruits (Figure 6a). Similar to the GA/ABA ratio, the IAA/ABA ratio increased rapidly upon imbibition: approximately 6-fold until day 5 in ungerminated fruits and almost doubling in day 5 germinated fruits (Figure 5d). As with GA, it appears that the endogenous IAA concentration on day 3 (approximately 0.1 nM) is sufficient for a full germination response of the entire population.

Treatment with the auxin transport (efflux) inhibitor 2,3,5-triiodobenzoic acid (TIBA) inhibited both embryo growth and germination of imbibed celery fruits (Figure 6d), suggesting roles for auxin transport in celery embryo growth and germination. By contrast, neither treatment with auxin biosynthesis inhibitors (Figure S6) nor with 0.1–10 μM IAA itself (Figure 6d) affected celery fruit germination. By contrast to 1–10 μM IAA which had no effect, 100 μM IAA significantly delayed germination by approximately 4 days (Figure 6d). Treatment with cytokinin (kinetin) had no effect (Figure 6d and Figure S6c). Taken together, these findings demonstrated that interactions between GAs, ABA and IAA are involved in embryo growth, endosperm degradation and germination of celery fruits.

Expression of storage resource and growth-related genes in germinating celery fruits

Expansins are proteins that facilitate cell wall extension, weakening and disassembly. Expansin genes are upregulated by GA and auxins during embryo and seedling cell growth and division, as well as during endosperm and fruit tissue weakening (Chen et al., 2001; de Farias et al., 2015;

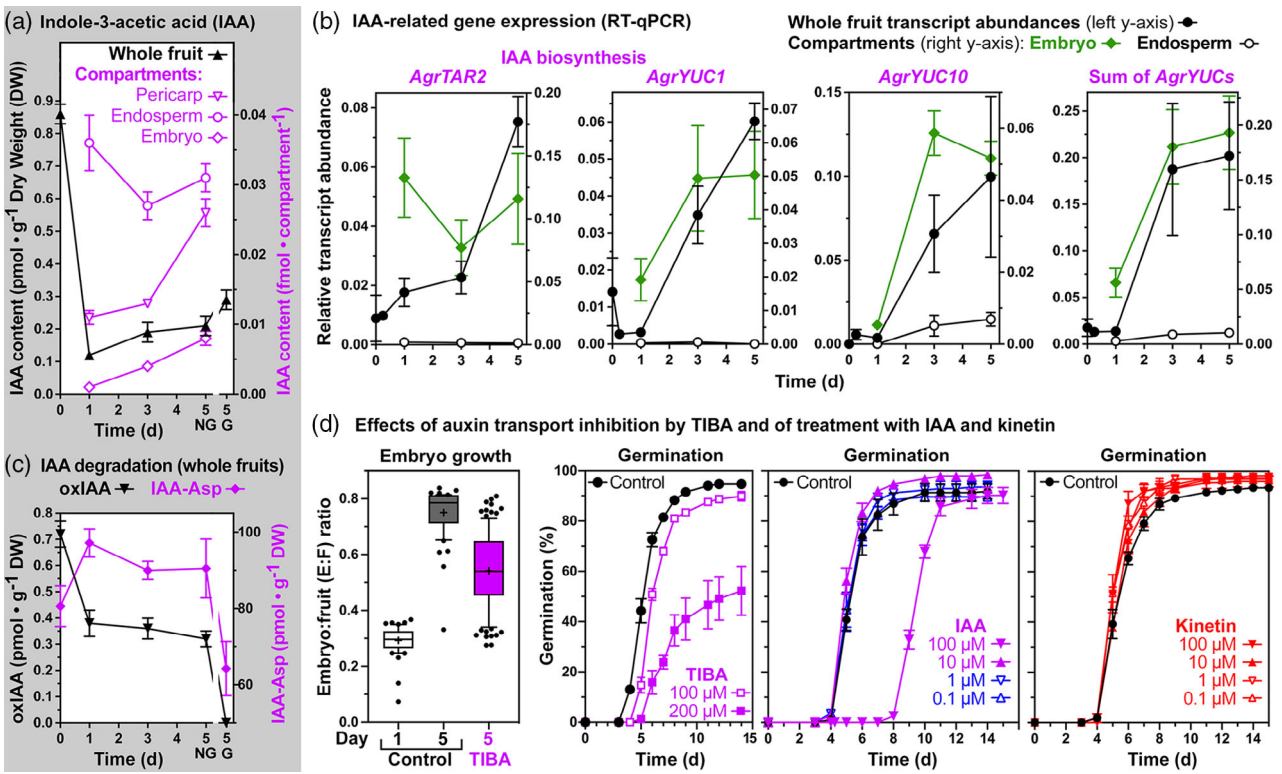

Figure 6. Auxin-related metabolite profiling, gene expression analysis and effects of treatments during embryo growth and germination of celery fruits. (a) Spatiotemporal patterns of the bioactive auxin indole-3-acetic acid (IAA) in *Apium graveolens* cv. Victoria during the incubation of imbibed fruits at 20°C in continuous light. (b) Whole fruit and compartment-specific relative transcript abundance patterns [reverse transcription quantitative real-time PCR (RT-qPCR)] during celery fruit imbibition in continuous light for key genes in the tryptophan-dependent IAA biosynthesis pathway: *TRYPTOPHAN AMINOTRANSFERASE RELATED 2* (*AgrTAR2*) and YUCCA (*AgrYUC1* and *AgrYUC2*); the sum of transcript abundances of all analysed YUCCA genes (both here and in Figure S4) is also presented. (c) Patterns of the major IAA degradation product 2-oxoindole-3-acetic acid (oxIAA) and the conjugated form IAA-aspartate (IAA-Asp). (d) Effects of the auxin transport inhibitor 2,3,5-triiodobenzoic acid (TIBA), IAA and kinetin on embryo growth and germination of fruits imbibed in continuous light. Box plots with 10–90 percentiles (embryo growth, approximately 50 embryos); the mean ± SEM values of five (metabolites) or three (RT-qPCR) biological replicate samples are presented; for further details, see Figure 4. NG, not germinated; G, germinated.

Ramakrishna et al., 2019; Valenzuela-Riffo et al., 2020). We identified two celery expansins that show contrasting transcript accumulation patterns in imbibed fruits (Figure 4g). The transcript abundance of *AgrEXPA2* was associated with the endosperm of dry fruits and declined approximately 9-fold during imbibition. By contrast, *AgrEXPA1* was very low in dry fruits and until day 1 (phase I), and subsequently accumulated approximately 130-fold on day 5. This accumulation of *AgrEXPA1* transcripts was localised in the endosperm, whereas roughly constant levels were expressed in the embryo (Figure 4g). Treatment with GA caused an earlier upregulation of *AgrEXPA1* expression approximately 4-fold already on day 1 (Figure S4c).

Storage compounds in the endosperm of celery (Figure S2) and other Apiaceae species are mainly proteins in protein bodies (aleurone grains) and triacylglycerol (oil) in oil bodies (Atia et al., 2012; Dwarte and Ashford, 1982; Kim and Janick, 1991; de Miranda et al., 2017; Ross and Murphy, 1992). Oleosins are oil body associated proteins involved in the synthesis of storage oil bodies during seed development (Huang, 1996). Consistent with the storage protein and oil body mobilisation and GA-induced endosperm degradation (Jacobsen and Pressman, 1979; Jacobsen et al., 1976), the *AgrOLEO* transcript abundance was high in dry celery fruit endosperm and fell rapidly upon imbibition (phase I) and further in phase II to 24-fold lower levels (Figure 4g). Treatment of celery fruits with GA promoted an earlier downregulation of the *AgrOLEO* transcript abundances, whereas ABA had no appreciable effect (Figure S4c).

Apiaceae store β-1,4-mannans as a major polysaccharide of their thick endosperm cell walls (Hopf and Kandler, 1977). Previous work with carrot showed that endo- β-1,4-mannanase enzyme activity and *DcMAN1* transcripts accumulate in the micropylar endosperm half of imbibed fruits in association with endosperm degradation and cavity formation for embryo growth (Homrichhausen et al., 2003). Figure 4g shows that the transcript abundance of *AgrMAN1*, the putative celery ortholog of *DcMAN1*, was low in dry fruits and until day 1 (phase I), but subsequently accumulated > 200-fold on day 3 during phase II. Expression of *AgrMAN1* was confined to the endosperm and essentially

absent in the embryo (Figure 4g). Treatment with GA caused an earlier upregulation of *AgrMAN1* expression, which was already > 30-fold on day 1 (Figure S4c). As for *DcMAN1* in carrot fruits (Homrichhausen et al., 2003), ABA did not appreciable affect the expression of *AgrMAN1* in celery fruits (Figure S4c). The ABA insensitivity, GA-inducibility and spatiotemporal expression patterns of *AgrMAN1* and *AgrEXPA1* are therefore consistent with their role in the GA-induced endosperm breakdown to facilitate the endosperm cavity formation for the embryo growth (Homrichhausen et al., 2003; Jacobsen et al., 1976) and the GA-induced weakening of the micropylar endosperm to facilitate radicle emergence (Bewley, 1997; Chen et al., 2001; de Farias et al., 2015; Nonogaki et al., 2000; Toorop et al., 2000).

In summary, reserve mobilisation and endosperm degradation controlled by interactions between GAs, ABA and IAA appear to regulate embryo growth within the seed and germination of celery fruits. In Figure 7 the patterns of hormone contents and related gene expression were compared between MD celery fruits and Brassicaceae seeds with either PD or ND. From these patterns, it is clear that the switch from a seed development to a germination programme occurs very early in phase I during celery fruit imbibition. The hormonal mechanisms, embryo–endosperm interactions and the spatiotemporal expression patterns of corresponding genes (Figure 7) demonstrate that the embryo growth inside the celery fruit is not simply the completion of embryogenesis or the post-embryogenesis embryo growth (compare with *A. thaliana* seed development and germination in Figure 7b) but instead a unique germination programme. The fruits of celery therefore constitute an excellent model system for investigating the underpinning mechanisms of MD as a distinct process.

DISCUSSION

Hormonally regulated embryo growth and endosperm breakdown are part of the unique germination programme of MD fruits

The majority of angiosperm species produce 'orthodox' diaspores in which drying during late maturation arrests the embryo in a quiescent state (Leprince et al., 2017; Nonogaki, 2019; Raz et al., 2001). The underdeveloped (small) embryos in dry celery fruits are fully differentiated with an established shoot-root body plan (Figures 2 and 3) (Dwarte and Ashford, 1982; Jacobsen et al., 1976; Jacobsen and Pressman, 1979). The mature fruits of celery and other Apiaceae have acquired desiccation tolerance during late maturation drying and also accumulated storage reserves in their mannan-rich endosperm (Atia et al., 2012; Dwarte and Ashford, 1982; Homrichhausen et al., 2003; Hopf and Kandler, 1977; Kim and Janick, 1991; de Miranda et al., 2017; Olszewski et al., 2005; Ross and Murphy, 1992; Shiota et al., 1998). We found that the contents of bioactive GAs (mainly GA_1), ABA and IAA, as well as their degradation products (GA_8 and GA_{29}, PA and DPA, oxIAA), are much higher in dry compared to imbibed celery fruits (Figures 4–6, Figure S4). This suggests that these hormones played important roles during Apiaceae seed development and that hormone degradation became dominant during late fruit development and maturation drying. In agreement with this, ABA accumulated as a transient peak [25–30 days after pollination (DAP)] during carrot seed development and declined during desiccation (40–60 DAP) (de Miranda et al., 2017; Shiota et al., 1998). Exogenous application of auxin during carrot reproduction enhanced the yield, size and quality of fruits, with increased germination percentages and vigour (Noor et al., 2020). Similarly, gibberellin or TIBA application reduced the germination percentages of *Heracleum sosnowskyi* (Koryzniene et al., 2019). Our work on celery and these examples from other Apiaceae MD/MPD fruits support the view that, as in PD/ND species, GA, ABA and IAA interact to control seed development, accumulate transiently during seed development and are degraded during late seed development (Figure 7). Embryogenesis in *A. thaliana* is completed at 7 DAP with the linear cotyledon (torpedo) embryo stage and is followed by a growth phase in which the embryo accumulates storage products and grows until it fills almost the entire seed at 13 DAP (Hu et al., 2018; Le et al., 2010; Raz et al., 2001). Figure 7 shows that IAA contents are high, with bioactive GAs and ABA increasing between 7 DAP and 9–10 DAP, and subsequently the levels of the three hormones decline and late maturation drying is dominated by hormone degradation (Hu et al., 2018; Kanno et al., 2010; Le et al., 2010; Okamoto et al., 2006; Pellizzaro et al., 2020). These patterns strongly suggest that the underdeveloped (small) embryos in celery and other Apiaceae fruits (Figure 1) do not simply resemble *A. thaliana* 7 DAP torpedo stage embryos. The subsequent embryo growth inside the fruit is therefore not simply the completion of embryogenesis or post-embryogenesis growth phase as occurs during *A. thaliana* seed development, but instead comprises a distinct process.

Celery fruit germination phase I (imbibition and induction) is associated with a rapid decline of bioactive GA, ABA and IAA levels (Figures 4–7). Although the ABA contents decline further, the GA and IAA contents increase slightly during phase II and the transition from phase II to III. The observed hormonal and gene expression patterns in imbibed celery fruits are consistent with this and highly similar to the germination of *A. thaliana* and *L. sativum*, representing PD and ND dormancy class seeds with large embryos. In all three systems, GA (*GA20ox*, *GA3ox*) and IAA (*YUC*) biosynthesis genes are upregulated in the embryo to produce bioactive GAs and IAA, whereas, in the

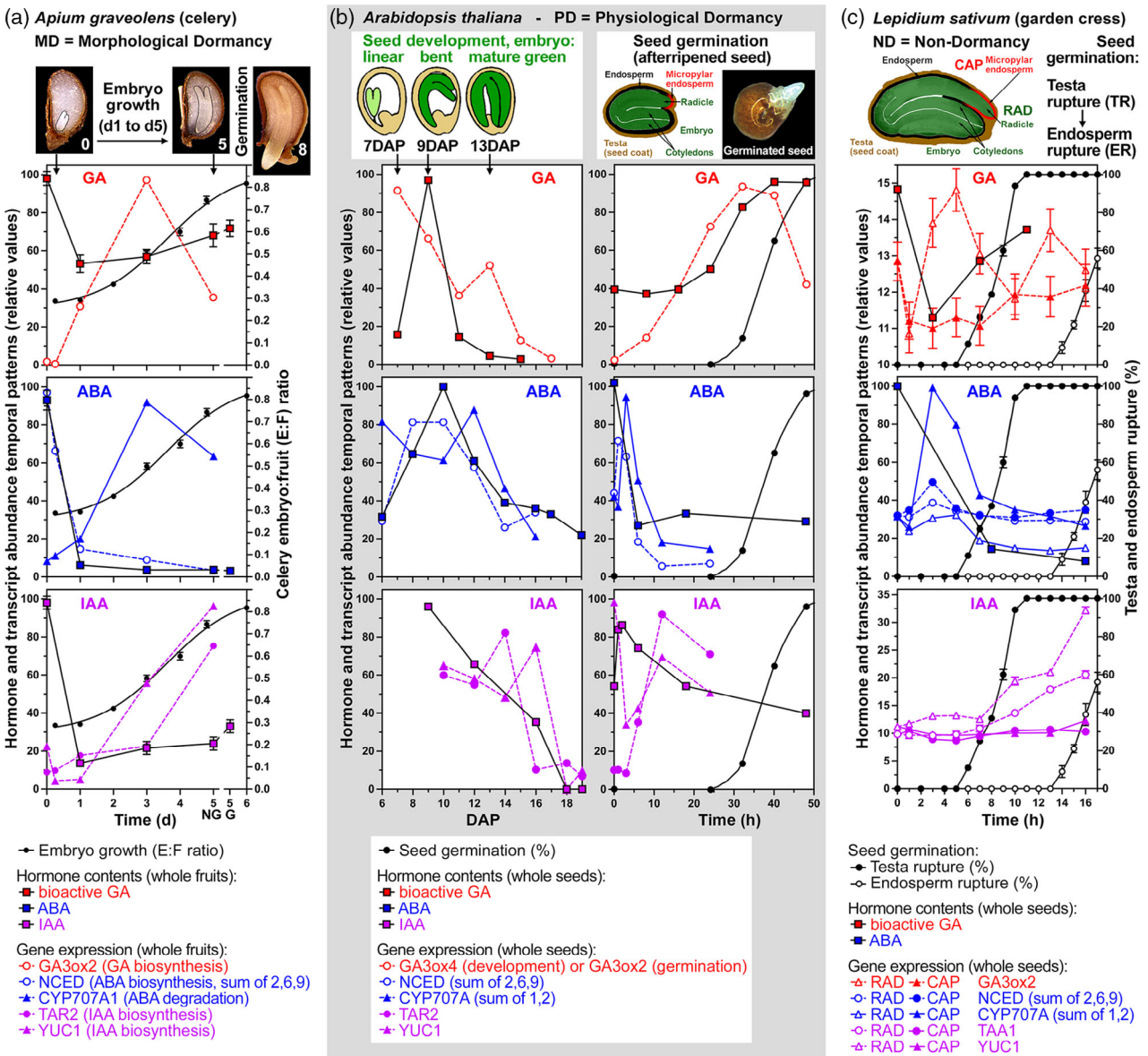

Figure 7. Comparison of the hormonal relations in Apiaceae and Brassicaceae seeds representing the dormancy classes morphological dormancy (MD), physiological dormancy (PD) and non-dormancy (ND), as indicated. Relative values for hormone contents and gene expression for bioactive gibberellins (GA), ABA and auxin (IAA, indole-3-acetic acid), as well as transcript expression patterns of major hormone biosynthesis genes, GA3ox (GA 3-oxidase), NCED (9-*cis*-epoxycarotenoid dioxygenase) and TAA1/TAR2/YUC1 (IAA biosynthesis, Figure S4a), in addition to ABA catabolism (CYP707A, ABA 8′-hydroxylase), are presented. (a) Hormone contents, gene expression and embryo growth (E:F ratios) during the germination of *Apium graveolens* (celery) fruits (relative values are calculated from absolute values, including those presented in Figures 4–6). (b) Hormone contents and gene expression during seed development and germination of *Arabidopsis thaliana*. Images on the top depict stages during late seed development (DAP, days after pollination) and germination as defined (Le et al., 2010; Weitbrecht et al., 2011). The results were compiled as follows: for seed development, bioactive GAs (GA_1+GA_3+GA_4) and *GA3ox4* (Hu et al., 2018), ABA (Wilhelmsson et al., 2019), *NCED* and CYP707A (Okamoto et al., 2006), IAA (Kanno et al., 2010) and *TAR2* and *YUC1* (Pellizzaro et al., 2020); for germination, bioactive GAs (GA_1+GA_4) (Ogawa et al., 2003), ABA (Chiwocha et al., 2005; Weitbrecht et al., 2011) and IAA (Chiwocha et al., 2005; Preston et al., 2009), with gene expression values from the Arabidopsis eFP Browser (Winter et al., 2007) for the experiments described (Nakabayashi et al., 2005; Preston et al., 2009). (c) Hormone contents and gene expression during the germination of non-dormant *Lepidium sativum* seeds. The results were compiled as follows: bioactive GAs (GA_1+GA_3+GA_4+GA_7) (Graeber et al., 2014) and ABA (Linkies et al., 2009), with gene expression values from Scheler et al. (2015). CAP, micropylar endosperm; RAD, radicle with the lower part of the hypocotyl (embryo growth zone).

case of ABA metabolism genes, upregulation of degradation (*CYP707A*) is mainly associated with the endosperm and downregulation of biosynthesis (*NCED*) is associated with both endosperm and embryo (Figures 4–7, Figures S4 and S6) (Chahtane et al., 2017; Chiwocha et al., 2005; Graeber et al., 2014; Kushiro et al., 2004; Lefebvre et al., 2006; Linkies et al., 2009; Ogawa et al., 2003; Preston et al., 2009; Scheler et al., 2015; Toh et al., 2008). In imbibed dormant

A. thaliana seeds (PD), *AtNCED6* and *AtNCED9* are upregulated to maintain dormancy by enhanced ABA biosynthesis (Ali-Rachedi et al., 2004; Chahtane et al., 2017; Lefebvre et al., 2006). The spatiotemporal expression patterns therefore support the view that embryo growth and endosperm breakdown within imbibed MD fruits constitute a unique germination programme. As during Brassicaceae seed germination, the three phases of celery fruit germination are controlled by increasing GA/ABA and IAA/ABA ratios and by changing tissue sensitivities to these hormones. For example, we found that the completion of germination by radicle protrusion is far more sensitive to inhibition by ABA compared to embryo growth within the fruit (Figure 4a-c). The estimated ABA sensitivity values of celery fruits [$ABA_b(50) = 375 \pm 0.91$ μM] (Figure 4) were similar to those obtained for tomato (288 ± 0.66 μM) (Ni and Bradford, 1992), *Brassica* (44–178 μM) (Still and Bradford, 1998) and barley (approximately 50 μM) (Bradford et al., 2008). Although these estimates describe the ABA sensitives of entire seeds or fruits, the importance of spatiotemporal differences was revealed for the embryo growth within celery fruits (Figure 4).

The GA-induced endosperm breakdown runs in parallel to embryo growth inside imbibed fruits of celery (Figures 2–4 and Dwarte and Ashford, 1982; Jacobsen et al., 1976; Jacobsen and Pressman, 1979) and other Apiaceae species (Atia et al., 2012; Cho et al., 2018; Homrichhausen et al., 2003; Oliva and Bradford, 1987; Olszewski et al., 2005). Many ND/PD eudicot species also retain abundant endosperm in their mature seeds, including tomato (Chen et al., 2001; Nonogaki et al., 2000; Toorop et al., 2000), tobacco (Manz et al., 2005) and others (Bewley, 1997). In these eudicot species and in MD coffee (de Farias et al., 2015; da Silva et al., 2008), the GA-induced mobilisation of oil and cell wall mannan mobilisation in the endosperm is not appreciably inhibited by ABA. This ABA-insensitive programme therefore differs in its hormonal regulation from the storage reserve mobilisation cereal grains endosperms, which is inhibited by ABA (Yan et al., 2014). In celery fruits, endosperm breakdown starts adjacent to the embryo and progresses radially, facilitating cavity formation (Figures 2 and 3) (Dwarte and Ashford, 1982; Jacobsen et al., 1976; Jacobsen and Pressman, 1979). This is achieved by GA-induced enzyme activities produced by the endosperm (autolysis) and neither IAA, ABA, ethylene nor kinetin can substitute for GA (Jacobsen et al., 1976). Degradation of the mannan-rich Apiaceae endosperm cell walls involves ABA-insensitive accumulation of *AgrMAN1* and *DcMAN1* in celery (Figure 6) and carrot (Homrichhausen et al., 2003), respectively. The expression of other endo-β-1,4-mannanases, as well as oil mobilisation in celery (Figure 5, Figure S4) and *Crithmum maritimum* (Atia et al., 2012), requires further research with respect to inhibition by ABA. ABA reduces GA-induced embryo growth and endosperm reserve mobilisation and strongly inhibits the completion of celery and carrot fruit germination (Figure 4, and Homrichhausen et al., 2003). The micropylar endosperm cells in celery fruits are especially sensitive to GA treatment, which leads to loss in tissue firmness and cell separation (Jacobsen et al., 1976). In both tomato (ND/PD) and coffee (MD), the micropylar endosperm weakening is biphasic, the first step is ABA-insensitive and the second step leading to radicle emergence is inhibited by ABA (Chen et al., 2001; de Farias et al., 2015; Nonogaki et al., 2000; da Silva et al., 2008; Toorop et al., 2000). The importance of micropylar restraint weakening (endosperm and pericarp) in celery fruits is clear (Figures S1,S3), although the mechanisms are unclear. Upon the embryo reaching the critical E:F ratio, ABA-sensitive micropylar endosperm weakening and pericarp rupture lead to completion of the MD germination programme by radicle emergence.

Apiaceae fruits as model systems to study the mechanisms of the ancestral morphological dormancy classes and the germination of underdeveloped embryos

The Apiaceae provide excellent model systems for investigating the mechanisms of MD/MPD. The Apieae tribe of the Apoideae subfamily is mainly characterized by species with MD but, within the genus *Apium*, there is also one species with MPD along with three species with MD (Figure 1, Data S1) (Burmeier and Jensen, 2008). Ecophysiological studies suggest a very close association between MD (small embryo, no physiological dormancy) and MPD (small embryo, physiological dormancy), and even single plants can produce both MD and MPD diaspores (Baskin and Baskin, 2014). Examples for this for Apiaceae include *Pastinaca sativa* and *Conium maculatum*, which, depending on the season or year, can produce mixtures of MD and MPD fruits (Baskin and Baskin, 1979, 1990); other examples are also shown (Figure 1, SI Methods, Data S1). For MPD fruits, additional pre-treatment to release the physiological dormancy block in phase I, thereby inducing embryo growth, usually takes several weeks of warm or cold stratification (Aihua et al., 2018; Baskin and Baskin, 2014; Cho et al., 2018; Porceddu et al., 2017; Zhang et al., 2019). In some of these species with MPD, the long stratification pre-treatment can be replaced by GA or fluridone (reducing ABA contents). On the other hand, MD celery fruit germination is light-requiring and only combined GA+fluridone treatment can replace the light to permit germination in darkness (Figures 3, 5g). The difference between stratification and light as a pre-treatment to remove blocks of physiological dormancy mechanisms (Finch-Savage and Leubner-Metzger, 2006) is that the long stratification simulates a 'slow natural signal' (a season), whereas light constitutes a more immediate 'fast natural signal' of spatial importance (e.g. position in soil). In either case, the importance of the GA/ABA balance for removing

the block from embryo growth in phase I is revealed. The observed increases in the GA/ABA and IAA/ABA ratios (Figure 5d) are mainly driven by ABA degradation.

We have revealed that several mechanisms traditionally associated with ND/PD seeds occur in Apiaceae fruits, which represent the ancestral MD/MPD diaspore classes with an underdeveloped embryo (Figures 1,2). The GA-ABA balance characteristic of PD (Finch-Savage and Leubner-Metzger, 2006; Nonogaki, 2019; Yan et al., 2014) and the shift in this balance that promotes PD release and germination is present in celery, although it is associated with the induction and progression of embryo growth within the fruit (Figures 3–5). A clear role for crosstalk between the embryo and the endosperm is apparent, with GA released by the embryo inducing responsive genes in the endosperm. Moreover, a biphasic nature of endosperm breakdown is apparent, with the main bulk of endosperm breakdown being less ABA-sensitive and associated with resource mobilisation to facilitate cavity formation and fuel embryo growth (phase II). By contrast, the late stage (phase III) is strongly ABA-sensitive to control radicle protrusion, probably by restraint weakening of the micropylar endosperm and pericarp, as is known for ND/PD seeds (Chahtane et al., 2017; Nonogaki, 2019; Steinbrecher and Leubner-Metzger, 2018; Yan et al., 2014).

Our work has revealed important roles for IAA not traditionally associated with PD seeds. In *A. thaliana* seeds, auxin controls seed dormancy through stimulation of ABA signalling (Liu et al., 2013) and is known as a key regulator of dormancy, longevity and maturation in PD seeds (Matilla, 2020; Pellizzaro et al., 2020; Shu et al., 2016). Auxin transport appears to be important for Apiaceae seed development (Koryzniene et al., 2019) and germination (Figure 6). Although IAA treatment did not appreciably affect celery germination under optimal conditions (Figure 6), it promoted dill fruit germination upon salt stress (Unver and Tilki, 2012) and enhanced the size, germination percentages and vigour of carrot fruits (Noor et al., 2020). IAA biosynthesis by the celery embryo plays a positive role in the control of its growth by cell expansion and division (Figure 7) (Van der Toorn and Karssen, 1992). It therefore appears that a complex interaction between GA, IAA and ABA metabolism, as well as changes in the tissue-specific sensitivities to these hormones, controls the unique germination programme of MD celery fruits. The embryo growth inside the fruit is not simply the completion of embryogenesis or *A. thaliana* equivalent post-embryogenesis growth but instead a distinct process, as revealed by the hormonal mechanisms, of embryo-endosperm interactions and spatiotemporal expression patterns of the corresponding genes (Figure 7). Our work with celery demonstrates that it is an excellent model system for MD fruits, whereas other Apiaceae with MPD fruits may be developed as models for the various levels of MPD.

EXPERIMENTAL PROCEDURES

Plant material and germination assays

The *Apium graveolens* L. cv. Victoria (celery) fruits used were harvested in 2014, maintained under company warehouse storage at 14°C with a relative humidity of 25% in foil bags and made available for the current research work in January 2017 by Tozer Seeds Ltd (Cobham, UK). The fruits of the Apiaceae are dry schizocarps that break into two dispersal units, which comprise single-seeded mericarps. In the present study, we use the term 'fruit' to refer to the mericarp. Germination assays were performed in a MLR-352 Environmental Test Chamber (Panasonic, Bracknell, UK) set to 20°C and with continuous white light (approximately 100 μmol s^{-1} m^{-2}). Triplicates of 50 fruits were used per treatment, with each triplicate sown into a Petri dish (diameter 6 cm) with two filter papers (MN713; Macherey-Nagel, Dueren, Germany) and 2 ml of autoclaved deionised water. Germination was defined as the visible emergence of the radicle through all the encasing tissues. Dose–response germination assays were performed using gibberellin A_{4+7} (GA_{4+7}; Duchefa Biochemie, Haarlem, The Netherlands), *cis,trans*-S(+)-ABA (Duchefa), flurprimidol (Sigma, St Louis, MO, USA), fluridone (Duchefa) and IAA (Sigma) at the indicated concentrations. These hormones and inhibitors were added to the germination assays from concentrated stock solutions with either water or, for GA_{4+7} and flurprimidol, DMSO as solvent. The germination curves of water and DMSO controls did not differ (Figure S5c). All treatments contained 0.1% plant preservative mixture (Plant Cell Technology, Washington, DC, USA).

Embryo growth assays and imaging

Internal embryo growth was assessed over the course of 6 days (at 0.25, 1, 2, 3, 4, 5 and 6 days), with the same incubation conditions as those used for the germination assays. Approximately 50 fruits were used per time point; to measure sizes, they were cut longitudinally and photographed using a DCF480 digital camera attached to a MZ 12.5 stereomicroscope (Leica, Wetzlar, Germany). The embryo and fruit lengths were measured via IMAGEJ, version 1.6.0 (National Institute of Health, Bethesda, MD, USA). Embryo (E) sizes were represented as a ratio of the fruit (F) length (E:F ratio) to account for the embryo-fruit size association. Germinated fruits were removed and their values replaced by a mean critical E:F ratio for radicle protrusion. The critical E:F ratio was calculated by measuring the internal embryo and fruit lengths of 50 fruits where the radicle had just protruded through the pericarp (<1/4 the length of the fruit). To quantify the embryo growth potential, fruits were imbibed for 1, 2, 3, 4 or 5 days using the same incubation conditions. At each time point, 48 embryos were extracted, photographed using the stereomicroscope and then incubated independently in 24-well plates lined with two filter papers (Whatman No. 1; GE Healthcare Life Sciences, Chicago, IL, USA) moistened with 150 μl of autoclaved deionised water. Embryos were photographed after a 9-day incubation period. Embryo lengths were measured using IMAGEJ. SRXTM 3D imaging was conducted as described previously (Arshad et al., 2020); for details, see SI Methods.

Plant hormone extraction and quantification

For whole fruit quantification of GAs, abscisates and auxins, Petri dishes of 50 fruits were imbibed as described for the germination assays. Five replicates were prepared for each time point, with approximately 100 fruits used per replicate sample. In addition to

whole fruit quantification at the 1-, 3- and 5-day time points, fruits were also separated into their three core compartments (endosperm, embryo and testa+pericarp) for tissue-specific hormone quantification of ABA and IAA. Approximately 150 endosperms, 450 pericarps, and between 3000 and 4000 embryos were used per sample, depending on the timepoint. The levels of 18 GAs, 3 ABA and 4 IAA pathway metabolites, physiologically active or non-active, were quantified as described previously (Flokova et al., 2014; Simura et al., 2018; Urbanova et al., 2013); for details, see SI Methods; for all results, see Table S1.

Reverse transcription quantitative real-time PCR (RT-qPCR)

Sampling was performed using the aforementioned germination conditions in triplicate. Whole fruits were sampled in the dry state (approximately 40 mg) and at 0.25, 1, 3 and 5 days of imbibition. For the fruit compartment samples, fruits were separated into the embryo and the remaining samples composed of the living endosperm plus the dead testa + pericarp tissues. For the 1-day imbibed samples, 600 embryos were extracted per sample; for the 3- and 5-day samples, 300 embryos were used. For the remaining samples, 200–300 were used per sample. RT-qPCR was conducted as in Graeber et al. (2011) with modifications and RNA extraction as described in detail in SI Methods and with the primer sequences listed in Table S2.

Statistical analysis

Germination data were compared through comparison of (1) final germination percentage, (2) germination uniformity and (3) germination rate (speed). Germination uniformity was defined as the time required for the middle 50% of germination to occur ($t_{75\%} - t_{25\%}$), whereas the germination rate was defined as the inverse of the time required for g % (with *g* being any number between 0 and 100) germination ($1/t_{g\%}$). These parameters were statistically compared using one-way analysis of variance (ANOVA). For the embryo growth data, E:F ratios were arcsine square root transformed for statistical testing. Non-linear regressions were fitted to the raw E:F ratio data sets and the hillslope coefficients were compared via one-way ANOVA. For all other statistical tests, data were compared using *t*-tests or the non-parametric Mann-Whitney test, where appropriate. All statistical analyses were performed using Prism, version 8.01 (GraphPad Software Inc., San Diego, CA, USA).

ACKNOWLEDGEMENTS

We thank Waheed Arshad and Lena Fatelnig for assistance with microscopy. We also thank Kent Bradford (University of California, Davis) for his expert advice and interesting discussions about hormone sensitivity modelling. We also acknowledge the Paul Scherrer Institut, Villigen, Switzerland, for provision of the synchrotron radiation beamtime (Proposal ID: 20180809; PI TS) at the TOMCAT beamline of the Swiss Light Source. This work was supported by Biotechnology and Biological Sciences Research Council (BBSRC) with a DTP iCASE training grant to MW (BB/M011178/1, project reference 1813810). The development of hormone analytics and molecular methods was further supported by the BBSRC Research Grants (BB/M02203X/1, BB/M00192X/1) to GL-M. The work was additionally supported from the European Regional Development Fund Project 'Plants as a tool for sustainable global development' (No. CZ.02.1.01/0.0/0.0/16_019/0000827) to MS and ON and 'Centre for Experimental Plant Biology' (No. CZ.02.1.01/0.0/0.0/16_019/0000738) to DT; the sample preparation and GA analysis was further supported by the Czech Science Foundation (grant no. 18-10349S) to DT.

CONFLICT OF INTEREST

The authors declare no conflict of interest.

AUTHOR CONTRIBUTIONS

MW, KN, MP, FG and GL-M planned and designed the research. MW, TS, FM and IP performed experiments. FG and MS provided access to materials. MW, KN, MP, TS, IP, ON, DT and GL-M analysed and interpreted data. MW, KN and GL-M wrote the manuscript with contributions from all of the authors.

DATA AVAILABILITY STATEMENT

All data presented or analysed in this published article are available online through figshare https://doi.org/10.17637/rh.14139821.v1

SUPPORTING INFORMATION

Additional Supporting Information may be found in the online version of this article.

Figure S1. Embryo growth and micropylar endosperm thickness in imbibed fruits of three *Apium graveolens* (celery) cultivars. (a) Progression of embryo growth inside the fruit and germination during incubation at 20°C in continuous light. Embryo growth within fruits was scored as embryo:fruit (E:F) ratios calculated from the embryo and fruit lengths. The critical E:F ratio represents the embryo growth threshold value at which radicle protrusion occurs. Mean values ± SEM are presented, N = 50. The sigmoidal non-linear regression curve fitted to the E:F ratio data had the indicated goodness of fit R^2 values and $P < 0.0001$. (b) Thickness of the micropylar endosperm in imbibed celery fruits. Mean values ± SEM are presented, N = 48. Note that linear regression analysis with the R^2 values indicated confirms that the thickness of the micropylar endosperm does not change between the start of imbibition and day 6. Significance was inferred using one-way ANOVA and found to be not significant.

Figure S2. Comparative SXRTM imaging of embryo growth within celery fruits. Digitally produced longitudinal sections of Synchrotron Radiation X-Ray Tomographic Microscopy (SXRTM) images of dry (a) and 5-day imbibed fruits (b). White boxes indicate the location of regions amplified in panels (c–f). Intact endosperm cells in dry fruits (c) compared to degraded endosperm cells adjacent to the growing embryo in 5-day imbibed fruits (d); note the reduction in the number of aleurone grains (AL) and the depleted endosperm cells. (e) Small embryo and micropylar endosperm region in dry fruits with dense cells in the radicle and embryonic shoot including the cotyledons. (f) Radicle and micropylar endosperm/pericarp region in 5-day imbibed fruits. The observed radicle tissue pattern as well as the cell size, shape and number, support that the embryo growth occurs by both cell expansion and division, this conclusion is consistent with earlier work (Van der Toorn and Karssen, 1992). The depleted area around the radicle is part of the endospermic cavity which the embryo induces to permit its growth within the fruit. Note further that the expected weakening of the micropylar endosperm during the 5-day imbibition is not associated with a change in the thickness of this tissue (for measurements see Figure S1) and that the

micropylar pericarp is a constraint to embryo emergence (see Figure S3).

Figure S3. Effect of pericarp removal on celery fruit germination. (a) Germination and calculated germination rates ($1/t_{50\%}$) of celery fruits imbibed (20°C in continuous light) with intact (control) pericarp or with a portion (as indicated) of the pericarp removed. (b) Germination and calculated germination uniformity ($t_{25\%}$–$t_{75\%}$) of celery fruits with intact pericarp or with a portion of the pericarp removed. Mean values ± SEM are presented, N = 50. Note that removal of the micropylar pericarp, but not the distal pericarp, affected celery fruit germination.

Figure S4. Expression analysis of hormone-related genes during embryo growth and germination of celery fruits. (a) Whole fruit and compartment-specific relative transcript abundance patterns (RT-qPCR) during celery fruit imbibition in continuous light at 20°C of GA- and ABA-related genes. The sum of *AgrNCED* transcripts was calculated from the results obtained for *AgrNCED2*, *ArgNCED6* (Figure 4) and *AgrNCED*9. (b) Spatiotemporal expression patterns of IAA-related genes. (c) Hormonal regulation of expansin, oleosin and endo-β-1,4-mannanase expression. Mean values ± SEM of 3 (RT-qPCR) biological replicate samples are presented; for further details see Figure 4.

Figure S5. Population-based threshold modelling of ABA effects on celery fruit germination. The theory behind these models is that the sensitivity threshold (or base) values for each hormone are normal distributed within the population and that hormone concentrations above these threshold values trigger dose responses over time which can be described by a hormone time constant (Bradford, 2005; Bradford et al., 2008; Bradford and Trewavas, 1994; Fennimore and Foley, 1998; Ni and Bradford, 1992, Still and Bradford, 1998). (a) Germination Rate (GR) analysis of ABA effects on the germination responses of celery fruits. The GR (g) values (speed of germination in 1/hour) are the inverse times to a specified germination percentage g and were derived for the percentages indicated from the obtained time courses (Figure 3b) of the individual germination dishes (each with 50 fruits) for each of the three replicates either without (control) or with ABA or fluridone added at the concentrations indicated. 1 μM ABA (10^{-6} M ABA) was identified as ABA_0, i.e., the highest ABA concentration having no effect on germination. To conduct the mathematical analysis, the 0.1 μM ABA and control which did not appreciably differ from ABA_0, were plotted just adjacent to the 1 μM ABA values (i.e. the 0.1 μM ABA was not plotted at it's 10^{-7} M position). As the next step the obtained slopes and x-axis interceptions were used to derive mean and median values indicative for the parameter of the targeted best-fitting base ABA concentrations ("ABA sensitivity") for each percentage g (ABA_b(g) in log[ABA]), standard deviation SD of mean log[ABA_b(50)], and the ABA time constant Θ_{ABA} (in log[ABA]·h). Repeated Probit analysis (see (b) and GR analysis of normalised ABA times (c) was conducted starting with the initial and variations of each of the three parameter (logABA_b(50), SD, Θ_{ABA}) until the best fitting values were obtained (R^2 values as indicators). These were then used to plot the lines presented in panel S5a. Responses to the various fluridone concentrations were included and placed at the log[ABA] position where they fit best. Note that for 10 μM fluridone this is for example at −6.8 (0.16 μM ABA) which is very close to the endogenous ABA concentration on day 3 (0.1 μM ABA). These ABA concentrations are well below values which act inhibitory (Figure 4c). (b) Repeated probit analysis delivered −3.43 (375 μM ABA) as the best-fitting log[ABA_b(50)] and from the slope of the best regression line (R^2 = 0.95) and −0.91 was derived as the best-fitting SD. (c) Using these parameter in GR analysis of normalized ABA time delivered Θ_{ABA} = −435 log[ABA]·h as the best estimate for the ABA time constant.

Figure S6. Auxin, cytokinin and ethylene related effects on celery fruit germination. (a) Simplified auxin metabolism and signalling with target sites of inhibitors indicated. (b) Spatiotemporal metabolite patterns of the major IAA degradation product 2-oxoindole-3-acetic acid (oxIAA) and the conjugated forms IAA-aspartic acid (IAA-Asp) and IAA-glutamate (IAA-Glu). Mean values ± SEM of 5 (metabolites) biological replicate samples are presented; for further details see Figure 5. (c) Effects of treatment with hormones and hormone-related 1inhibitors on the germination of celery fruits imbibed at 20°C in continuous light. Mean values ± SEM of three plates each with 50 fruits are presented. Note that very low IAA concentrations (0.05–0.5 nM) may have a minor promoting effect and that 100 μM IAA significantly delayed celery fruit germination by ca. 4 days. A similar delay was observed with 100 μM of the ethylene precursor 1-aminocyclopropane-1-carboxylic acid (ACC) suggesting that auxin-ethylene may also be involved.

Table S1. Hormone metabolite contents in celery fruits.

Table S2. Primer sequences used for RT-qPCR.

Data S1. Apiaceae MD and MPD distribution analysis.

REFERENCES

Aihua, L., Shunyuan, J., Guang, Y., Ying, L., Na, G., Tong, C. *et al.* (2018) Molecular mechanism of seed dormancy release induced by fluridone compared with cold stratification in *Notopterygium incisum*. *BMC Plant Biology*, **18**, 116.

Ali-Rachedi, S., Bouinot, D., Wagner, M.H., Bonnet, M., Sotta, B., Grappin, P. *et al.* (2004) Changes in endogenous abscisic acid levels during dormancy release and maintenance of mature seeds: studies with the Cape Verde Islands ecotype, the dormant model of *Arabidopsis thaliana*. *Planta*, **219**, 479–488.

Arshad, W., Marone, F., Collinson, M.E., Leubner-Metzger, G. & Steinbrecher, T. (2020) Fracture of the dimorphic fruits of *Aethionema arabicum* (Brassicaceae). *Botany-Botanique*, **98**, 65–75.

Atia, A., Debez, A., Barhoumi, Z., Abdelly, C. & Smaoui, A. (2012) Investigation of embryo growth and reserve mobilization of water or salt imbibed seeds of *Crithmum maritimum* L. *Acta Botanica Gallica*, **159**, 17–24.

Baskin, C.C. & Baskin, J.M. (2014) *Seeds—Ecology, biogeography, and evolution of dormancy and germination* San Diego. London: Academic Press.

Baskin, J.M. & Baskin, C.M. (1979) Studies on the autecology and population biology of the weedy monocarpic perennial, *Pastinaca sativa*. *Journal of Ecology*, **67**, 601–610.

Baskin, J.M. & Baskin, C.C. (1990) Seed germination ecology of poison hemlock, *Conium maculatum*. *Canadian Journal of Botany*, **68**, 2018–2024.

Baskin, J.M., Hidayati, S.N., Baskin, C.C., Walck, J.L., Huang, Z.Y. & Chien, C.T. (2006) Evolutionary considerations of the presence of both morphophysiological and physiological seed dormancy in the highly advanced euasterids II order Dipsacales. *Seed Science Research*, **16**, 233–242.

Bewley, J.D. (1997) Breaking down the walls—a role for endo-ß-mannanase in release from seed dormancy ? *Trends in Plant Science*, **2**, 464–469.

Bradford, K.J. (2005) Threshold models applied to seed germination ecology. *New Phytologist*, **165**, 338–341.

Bradford, K.J., Benech-Arnold, R.L., Come, D. & Corbineau, F. (2008) Quantifying the sensitivity of barley seed germination to oxygen, abscisic acid, and gibberellin using a population-based threshold model. *Journal of Experimental Botany*, **59**, 335–347.

Bradford, K.J. & Trewavas, J. (1994) Sensitivity thresholds and variable time scales in plant hormone action. *Plant Physiology*, **105**, 1029–1036.

Burmeier, S. & Jensen, K. (2008) Is the endangered *Apium repens* (Jacq.) Lag. rare because of a narrow regeneration niche? *Plant Species Biology*, **23**, 111–118.

Calvino, C.I., Teruel, F.E. & Downie, S.R. (2016) The role of the Southern Hemisphere in the evolutionary history of Apiaceae, a mostly north temperate plant family. *Journal of Biogeography*, **43**, 398–409.

Cao, J.S., Li, G.J., Qu, D.J., Li, X. & Wang, Y.N. (2020) Into the seed: auxin controls seed development and grain yield. *International Journal of Molecular Sciences*, **21**, 1662.

Chahtane, H., Kim, W. & Lopez-Molina, L. (2017) Primary seed dormancy: a temporally multilayered riddle waiting to be unlocked. *Journal of Experimental Botany*, **68**, 857–869.

Chen, F., Dahal, P. & Bradford, K.J. (2001) Two tomato expansin genes show divergent expression and localization in embryos during seed development and germination. *Plant Physiology*, **127**, 928–936.

Chiwocha, S.D.S., Cutler, A.J., Abrams, S.R., Ambrose, S.J., Yang, J., Ross, A.R.S. *et al.* (2005) The *etr1-2* mutation in *Arabidopsis thaliana* affects the abscisic acid, auxin, cytokinin and gibberellin metabolic pathways during maintenance of seed dormancy, moist-chilling and germination. *The Plant Journal*, **42**, 35–48.

Cho, J.S., Jang, B.K. & Lee, C.H. (2018) Seed dormancy and germination characteristics of the endangered species *Cicuta virosa* L. in South Korea. *Horticulture, Environment, and Biotechnology*, **59**, 473–481.

da Silva, E.A., Toorop, P.E., Van Lammeren, A.A. & Hilhorst, H.W. (2008) ABA inhibits embryo cell expansion and early cell division events during coffee (*Coffea arabica* 'Rubi') seed germination. *Annals of Botany*, **102**, 425–433.

de Farias, E.T., da Silva, E.A.A., Toorop, P.E., Bewley, J.D. & Hilhorst, H.W.M. (2015) Expression studies in the embryo and in the micropylar endosperm of germinating coffee (*Coffea arabica* cv. Rubi) seeds. *Plant Growth Regulation*, **75**, 575–581.

de Miranda, R.M., Dias, D.C.F.D., Picoli, E.A.D., da Silva, P.P. & Nascimento, W.M. (2017) Physiological quality, anatomy and histochemistry during the development of carrot seeds (*Daucus carota* L.). *Ciência e Agrotecnologia*, **41**, 169–180.

Dwarte, D. & Ashford, A.E. (1982) The chemistry and microstructure of protein bodies in celery endosperm. *Botanical Gazette*, **143**, 164–175.

Fennimore, S.A. & Foley, M.E. (1998) Genetic and physiological evidence for the role of gibberellic acid in the germination of dormant Avena fatua seeds. *Journal of Experimental Botany*, **49**, 89–94.

Fernandez-Pascual, E., Mattana, E. & Pritchard, H.W. (2019) Seeds of future past: climate change and the thermal memory of plant reproductive traits. *Biological Reviews*, **94**, 439–456.

Finch-Savage, W.E. & Footitt, S. (2017) Seed dormancy cycling and the regulation of dormancy mechanisms to time germination in variable field environments. *Journal of Experimental Botany*, **68**, 843–856.

Finch-Savage, W.E. & Leubner-Metzger, G. (2006) Seed dormancy and the control of germination. *New Phytologist*, **171**, 501–523.

Flokova, K., Tarkowska, D., Miersch, O., Strnad, M., Wasternack, C. & Novak, O. (2014) UHPLC-MS/MS based target profiling of stress-induced phytohormones. *Phytochem*, **105**, 147–157.

Forbis, T.A., Floyd, S.K. & deQueiroz, A. (2002) The evolution of embryo size in angiosperms and other seed plants: Implications for the evolution of seed dormancy. *Evolution*, **56**, 2112–2125.

Friis, E.M., Crane, P.R., Pedersen, K.R., Stampanoni, M. & Marone, F. (2015) Exceptional preservation of tiny embryos documents seed dormancy in early angiosperms. *Nature*, **528**, 551–554.

Graeber, K., Linkies, A., Steinbrecher, T., Mummenhoff, K., Tarkowská, D., Turečková, V. *et al.* (2014) *DELAY OF GERMINATION 1* mediates a conserved coat dormancy mechanism for the temperature- and gibberellin-dependent control of seed germination. *Proceedings of the National Academy of Sciences of the United States of America*, **111**, E3571–E3580.

Graeber, K., Linkies, A., Wood, A.T. & Leubner-Metzger, G. (2011) A guideline to family-wide comparative state-of-the-art quantitative RT-PCR analysis exemplified with a Brassicaceae cross-species seed germination case study. *The Plant Cell*, **23**, 2045–2063.

Holloway, T., Steinbrecher, T., Perez, M., Seville, A., Stock, D., Nakabayashi, K. *et al.* (2021) Coleorhiza-enforced seed dormancy: a novel mechanism to control germination in grasses. *New Phytologist*, **229**, 2179–2191.

Homrichhausen, T.M., Hewitt, J.R. & Nonogaki, H. (2003) Endo-ß-mannanase activity is associated with the completion of embryogenesis in imbibed carrot (*Daucus carota* L.) seeds. *Seed Science Research*, **13**, 219–227.

Hopf, H. & Kandler, O. (1977) Characterization of reserve cellulose of endosperm of *Carum carvi* as a beta-(1–4)-mannan. *Phytochem*, **16**, 1715–1717.

Hu, Y.L., Zhou, L.M., Huang, M.K., He, X.M., Yang, Y.H., Liu, X. *et al.* (2018) Gibberellins play an essential role in late embryogenesis of Arabidopsis. *Nature Plants*, **4**, 289–298.

Huang, A.H. (1996) Oleosins and oil bodies in seeds and other organs. *Plant Physiology*, **110**, 1055–1061.

Jacobsen, J.V. & Pressman, E. (1979) A structural study of germination in celery (*Apium graveolens* L.) seed with emphasis on endosperm breakdown. *Planta*, **144**, 241–248.

Jacobsen, J.V., Pressman, E. & Pyliotis, N.A. (1976) Gibberellin-induced separation of cells in isolated endosperm of celery seed. *Planta*, **129**, 113–122.

Kanno, Y., Jikumaru, Y., Hanada, A., Nambara, E., Abrams, S.R., Kamiya, Y. *et al.* (2010) Comprehensive hormone profiling in developing Arabidopsis seeds: examination of the site of ABA biosynthesis, ABA transport and hormone interactions. *Plant and Cell Physiology*, **51**, 1988–2001.

Kasahara, H. (2016) Current aspects of auxin biosynthesis in plants. *Bioscience Biotechnology and Biochemistry*, **80**, 34–42.

Kim, Y.H. & Janick, J. (1991) Abscisic acid and proline improve desiccation tolerance and increase fatty acid content of celery somatic embryos. *Plant Cell Tissue and Organ Culture*, **24**, 83–89.

Koryzniene, D., Jurkoniene, S., Zalnierius, T., Gaveliene, V., Jankovska-Bortkevic, E., Bareikiene, N. *et al.* (2019) *Heracleum sosnowskyi* seed development under the effect of exogenous application of GA_3. *PeerJ*, **7**, ARTN e6906.

Kushiro, T., Okamoto, M., Nakabayashi, K., Yamagishi, K., Kitamura, S., Asami, T. *et al.* (2004) The *Arabidopsis* cytochrome P450 CYP707A encodes ABA 8′-hydroxylases: key enzymes in ABA catabolism. *European Molecular Biology Organization Journal*, **23**, 1647–1656.

Le, B.H., Cheng, C., Bui, A.Q., Wagmaister, J.A., Henry, K.F., Pelletier, J. *et al.* (2010) Global analysis of gene activity during Arabidopsis seed development and identification of seed-specific transcription factors. *Proceedings of the National Academy of Sciences of the United States of America*, **107**, 8063–8070.

Lefebvre, V., North, H., Frey, A., Sotta, B., Seo, M., Okamoto, M. *et al.* (2006) Functional analysis of Arabidopsis *NCED6* and *NCED9* genes indicates that ABA synthesized in the endosperm is involved in the induction of seed dormancy. *The Plant Journal*, **45**, 309–319.

Leprince, O., Pellizzaro, A., Berriri, S. & Buitink, J. (2017) Late seed maturation: drying without dying. *Journal of Experimental Botany*, **68**, 827–841.

Li, H.T., Yi, T.S., Gao, L.M., Ma, P.F., Zhang, T., Yang, J.B. *et al.* (2019) Origin of angiosperms and the puzzle of the Jurassic gap. *Nature Plants*, **5**, 461–470.

Li, M.Y., Feng, K., Hou, X.L., Jiang, Q., Xu, Z.S., Wang, G.L. *et al.* (2020) The genome sequence of celery (*Apium graveolens* L.), an important leaf vegetable crop rich in apigenin in the Apiaceae family. *Horticulture Research*, **7**, ARTN 9.

Linkies, A., Müller, K., Morris, K., Turečková, V., Cadman, C.S.C., Corbineau, F. *et al.* (2009) Ethylene interacts with abscisic acid to regulate endosperm rupture during germination: a comparative approach using *Lepidium sativum* and *Arabidopsis thaliana*. *The Plant Cell*, **21**, 3803–3822.

Liu, X.D., Zhang, H., Zhao, Y., Feng, Z.Y., Li, Q., Yang, H.Q. *et al.* (2013) Auxin controls seed dormancy through stimulation of abscisic acid signaling by inducing ARF-mediated ABI3 activation in Arabidopsis. *Proceedings of the National Academy of Sciences of the United States of America*, **110**, 15485–15490.

MacGregor, D.R., Kendall, S.L., Florance, H., Fedi, F., Moore, K., Paszkiewicz, K. *et al.* (2015) Seed production temperature regulation of primary dormancy occurs through control of seed coat phenylpropanoid metabolism. *New Phytologist*, **205**, 642–652.

Manz, B., Müller, K., Kucera, B., Volke, F. & Leubner-Metzger, G. (2005) Water uptake and distribution in germinating tobacco seeds investigated *in vivo* by nuclear magnetic resonance imaging. *Plant Physiology*, **138**, 1538–1551.

Martin, A.C. (1946) The comparative internal morphology of seeds. *The American Midland Naturalist*, **36**, 513–660.

Matilla, A.J. (2020) Auxin: hormonal signal required for seed development and dormancy. *Plants (Basel)*, **9**, 705.

Nakabayashi, K., Okamoto, M., Koshiba, T., Kamiya, Y. & Nambara, E. (2005) Genome-wide profiling of stored mRNA in *Arabidopsis thaliana* seed germination: epigenetic and genetic regulation of transcription in seed. *The Plant Journal*, **41**, 697–709.

Ni, B.-R. & Bradford, K.J. (1992) Quantitative models characterizing seed germination responses to abscisic acid and osmoticum. *Plant Physiology*, **98**, 1057–1068.

Nonogaki, H. (2019) Seed germination and dormancy: The classic story, new puzzles, and evolution. *Journal of Integrative Plant Biology*, **61**, 541–563.

Nonogaki, H., Gee, O.H. & Bradford, K.J. (2000) A germination-specific endo-ß-mannanase gene is expressed in the micropylar endosperm cap of tomato seeds. *Plant Physiology*, **123**, 1235–1245.

Noor, A., Ziaf, K., Amjad, M. & Ahmad, I. (2020) Synthetic auxins concentration and application time modulates seed yield and quality of carrot by altering the umbel order. *Sci Hortic-Amsterdam*, **262**, 109066.

Ogawa, M., Hanada, A., Yamauchi, Y., Kuwahara, A., Kamiya, Y. & Yamaguchi, S. (2003) Gibberellin biosynthesis and response during *Arabidopsis* seed germination. *The Plant Cell*, **15**, 1591–1604.

Okamoto, M., Kuwahara, A., Seo, M., Kushiro, T., Asami, T., Hirai, N. *et al.* (2006) *CYP707A1* and *CYP707A2*, which encode ABA 8′-hydroxylases, are indispensable for a proper control of seed dormancy and germination in Arabidopsis. *Plant Physiology*, **141**, 97–107.

Oliva, R.N. & Bradford, K.J. (1987) Seed quality in carrots (*Daucus carota* L.) —influence of plant spacing and umbel order. *HortScience*, **22**, 1127.

Olszewski, M., Pill, W., Pizzolato, T.D. & Pesek, J. (2005) Priming duration influences anatomy and germination responses of parsley mericarps. *Journal of the American Society for Horticultural Science*, **130**, 754–758.

Pellizzaro, A., Neveu, M., Lalanne, D., Vu, B.L., Kanno, Y., Seo, M. *et al.* (2020) A role for auxin signaling in the acquisition of longevity during seed maturation. *New Phytologist*, **225**, 284–296.

Porceddu, M., Mattana, E., Pritchard, H.W. & Bacchetta, G. (2017) Dissecting seed dormancy and germination in *Aquilegia barbaricina*, through thermal kinetics of embryo growth. *Plant Biology*, **19**, 983–993.

Preston, J., Tatematsu, K., Kanno, Y., Hobo, T., Kimura, M., Jikumaru, Y. *et al.* (2009) Temporal expression patterns of hormone metabolism genes during imbibition of *Arabidopsis thaliana* seeds: a comparative study on dormant and non-dormant accessions. *Plant and Cell Physiology*, **50**, 1786–1800.

Ramakrishna, P., Ruiz Duarte, P., Rance, G.A., Schubert, M., Vordermaier, V., Vu, L.D. *et al.* (2019) EXPANSIN A1-mediated radial swelling of pericycle cells positions anticlinal cell divisions during lateral root initiation. *Proceedings of the National Academy of Sciences of the United States of America*, **116**, 8597–8602.

Raz, V., Bergervoet, J.H.W. & Koornneef, M. (2001) Sequential steps for developmental arrest in Arabidopsis seeds. *Development*, **128**, 243–252.

Ross, J.H.E. & Murphy, D.J. (1992) Biosynthesis and localization of storage proteins, oleosins and lipids during seed development in *Coriandrum sativum* and other Umbelliferae. *Plant Science*, **86**, 59–70.

Scheler, C., Weitbrecht, K., Pearce, S.P., Hampstead, A., Buettner-Mainik, A., Lee, K. *et al.* (2015) Promotion of testa rupture during garden cress germination involves seed compartment-specific expression and activity of pectin methylesterases. *Plant Physiology*, **167**, 200–215.

Shiota, H., Satoh, R., Watabe, K., Harada, H. & Kamada, H. (1998) *C-ABI3*, the carrot homologue of the Arabidopsis *ABI3*, is expressed during both zygotic and somatic embryogenesis and functions in the regulation of embryo-specific ABA-inducible genes. *Plant and Cell Physiology*, **39**, 1184–1193.

Shu, K., Liu, X.D., Xie, Q. & He, Z.H. (2016) Two faces of one seed: hormonal regulation of dormancy and germination. *Molecular Plant*, **9**, 34–45.

Simura, J., Antoniadi, I., Siroka, J., Tarkowska, D., Strnad, M., Ljung, K. *et al.* (2018) Plant hormonomics: multiple phytohormone profiling by targeted metabolomics. *Plant Physiology*, **177**, 476–489.

Steinbrecher, T. & Leubner-Metzger, G. (2018) Tissue and cellular mechanics of seeds. *Current Opinion in Genetics & Development*, **51**, 1–10.

Still, D.W. & Bradford, K.J. (1998) Using hydrotime and ABA-time models to quantify seed quality of Brassicas during development. *Journal of the American Society for Horticultural Science*, **123**, 692–699.

Toh, S., Imamura, A., Watanabe, A., Nakabayashi, K., Okamoto, M., Jikumaru, Y. *et al.* (2008) High temperature-induced abscisic acid biosynthesis and its role in the inhibition of gibberellin action in Arabidopsis seeds. *Plant Physiology*, **146**, 1368–1385.

Toorop, P.E., van Aelst, A.C. & Hilhorst, H.W.M. (2000) The second step of the biphasic endosperm cap weakening that mediates tomato (*Lycopersicon esculentum*) seed germination is under control of ABA. *Journal of Experimental Botany*, **51**, 1371–1379.

Unver, M.C. & Tilki, F. (2012) Salinity, germination promoting chemicals, temperature and light effects on seed germination of *Anethum graveolens* L. *Bulgarian Journal of Agricultural Science*, **18**, 1005–1011.

Urbanova, T., Tarkowska, D., Novak, O., Hedden, P. & Strnad, M. (2013) Analysis of gibberellins as free acids by ultra performance liquid chromatography-tandem mass spectrometry. *Talanta*, **112**, 85–94.

Valenzuela-Riffo, F., Parra-Palma, C., Ramos, P. & Morales-Quintana, L. (2020) Molecular and structural insights into FaEXPA5, an alpha-expansin protein related with cell wall disassembly during ripening of strawberry fruit. *Plant Physiology and Biochemistry*, **154**, 581–589.

Van der Toorn, P. & Karssen, C.M. (1992) Analysis of embryo growth in mature fruits of celery (*Apium graveolens*). *Plysiologia Plantarum*, **84**, 593–599.

Vandelook, F., Janssens, S.B. & Probert, R.J. (2012) Relative embryo length as an adaptation to habitat and life cycle in Apiaceae. *New Phytologist*, **195**, 479–487.

Weitbrecht, K., Müller, K. & Leubner-Metzger, G. (2011) First off the mark: early seed germination. *Journal of Experimental Botany*, **62**, 3289–3309.

Wen, J., Yu, Y., Xie, D.F., Peng, C., Liu, Q., Zhou, S.D. *et al.* (2020) A transcriptome-based study on the phylogeny and evolution of the taxonomically controversial subfamily Apioideae (Apiaceae). *Annals of Botany*, **125**, 937–953.

Wilhelmsson, P.K.I., Chandler, J.O., Fernandez-Pozo, N., Graeber, K., Ullrich, K.K., Arshad, W. *et al.* (2019) Usability of reference-free transcriptome assemblies for detection of differential expression: a case study on *Aethionema arabicum* dimorphic seeds. *BMC Genomics*, **20**, ARTN 95.

Willis, C.G., Baskin, C.C., Baskin, J.M., Auld, J.R., Venable, D.L., Cavender-Bares, J. *et al.* (2014) The evolution of seed dormancy: environmental cues, evolutionary hubs, and diversification of the seed plants. *New Phytologist*, **203**, 300–309.

Winter, D., Vinegar, B., Nahal, H., Ammar, R., Wilson, G.V. & Provart, N.J. (2007) An "electronic fluorescent pictograph" browser for exploring and analyzing large-scale biological data sets. *PLoS One*, **2**, e718.

Yan, D., Duermeyer, L., Leoveanu, C. & Nambara, E. (2014) The functions of the endosperm during seed germination. *Plant and Cell Physiology*, **55**, 1521–1533.

Zhang, K.L., Yao, L.J., Zhang, Y., Baskin, J.M., Baskin, C.C., Xiong, Z.M. *et al.* (2019) A review of the seed biology of *Paeonia* species (Paeoniaceae), with particular reference to dormancy and germination. *Planta*, **249**, 291–303.